

# MULTIPLE CRITERIA OPTIMIZATION IN INJECTION MOLDING

A Thesis

Presented in Partial Fulfillment of the Requirements for

Graduation with Distinction in the

Department of Mechanical Engineering at

The Ohio State University

By

Carlos Castro

\*\*\*\*\*

The Ohio State University

2004

Honors Thesis Committee:

Dr. Blaine Lilly, Advisor

Dr. Mark Walter

**Abstract:**

Injection molding (IM) is considered the most prominent processes for mass-producing plastic products. One of the biggest challenges facing injection molders today is to determine the proper settings for the IM process variables. Selecting the proper settings for an IM process is crucial because the behavior of the polymeric material during shaping is highly influenced by the process variables. Consequently, the process variables govern the quality of the part produced. The difficulty of optimizing an IM process is that the performance measures-quantities that characterize the adequacy of part, process, or machine to intended purposes such, i.e. surface quality or cycle time-usually show conflicting behavior. Therefore, a compromise must be found between all of the performance measures of interest. This thesis demonstrates a method incorporating Computer Aided Engineering, Artificial Neural Networks, and Data Envelopment Analysis (DEA) that can be used to find the best compromises between performance measures in IM, and potentially other polymer processes.

## Table of Contents

<b>Chapter 1: Introduction and Research Objectives</b> .....	1
1.1 Introduction.....	1
1.2 Research Objective.....	4
<b>Chapter 2: Methodology</b> .....	5
2.1 The Optimization Strategy.....	5
2.2 Experimental Methodology.....	7
<b>Chapter 3: Technical Background</b> .....	11
3.1 Injection Molding Background.....	11
3.2 Metamodeling.....	13
3.2.1 Linear Regression Models.....	13
3.2.2 Artificial Neural Networks.....	14
3.3 Data Envelopment Analysis Background.....	17
<b>Chapter 4: Results</b> .....	21
4.1 Metamodeling Results.....	21
4.2 Data Envelopment Analysis Results.....	24
4.3 Analysis of Robust Solutions.....	42
<b>Chapter 5: Conclusions and Future Work</b> .....	44
5.1 Conclusions.....	44
5.2 Future Work.....	44
<b>References</b> .....	46
<b>Appendix I: Initial dataset from Moldflow simulations</b> .....	47

## LIST OF FIGURES

<b>Figure 1.1:</b> Schematic of the virtual part with constant thickness and window frame cutouts.....	3
<b>Figure 2.1:</b> Schematic of the Optimization Strategy.....	5
<b>Figure 2.2:</b> Schematic to define how $t_A$ , $t_B$ , $t_{oe}$ , $d_1$ , and $d_2$ were found.....	8
<b>Figure 3.1:</b> Typical reciprocating screw injection molding machine [4].....	11
<b>Figure 3.2:</b> Pressure at injection location for on cycle of injection molding [4].....	12
<b>Figure 3.3:</b> Schematic of an artificial neural network with three inputs, two neurons in the hidden layer, and two outputs.....	15
<b>Figure 3.4:</b> Sample dataset with the efficient frontier shown.....	18
<b>Figure 4.1:</b> Levels of the PMs that corresponded to the efficient solutions when all nine were included.....	25
<b>Figure 4.2:</b> Efficient solutions for the excess machine capacity application in terms of the levels of the PMs considered.....	27
<b>Figure 4.3:</b> Injection locations of the efficient solutions to the excess machine capacity application transformed to fall between -1 and 1.....	28
<b>Figure 4.4:</b> A visualization of the efficient frontier of the economics critical and dimensional application.....	30
<b>Figure 4.5:</b> Efficient Solutions for the economics critical and dimensional application in terms of the PMs considered.....	31
<b>Figure 4.6:</b> Injection location of the efficient solutions to the dimensional quality and economics critical application transformed to fall between -1 and 1.....	32
<b>Figure 4.7:</b> Visualization of the efficient frontier in the structural application.....	34
<b>Figure 4.8:</b> Efficient solutions for the structural application in terms of the weld line positions $d_1$ and $d_2$ .....	35

<b>Figure 4.9:</b> Injection locations of the seven efficient solutions to the structural application transformed to fall between -1 and 1.....	36
<b>Figure 4.10:</b> Visualization of the efficient frontier for the part quality application..	37
<b>Figure 4.11:</b> Efficient solutions for the part quality application in terms of the positions of the weld lines and deflection range.....	38
<b>Figure 4.12:</b> Injection Locations of the seven efficient solutions to the part quality application transformed to fall between -1 and 1.....	39
<b>Figure 4.13:</b> Efficient solutions for the case of determining the injection location in terms of the levels the PMs considered.....	41
<b>Figure 4.14:</b> Injection locations of the efficient solutions for the application considering only $x,y$ dependent PMs.....	42

## LIST OF TABLES

<b>Table 2.1:</b> Levels of controllable variables used to obtain initial experimental data..	7
<b>Table 2.2:</b> Levels of controllable variables for the validation dataset.....	9
<b>Table 2.3:</b> Levels of the controllable variables for the dataset that was the subject of the Multiple Criteria Optimization.....	10
<b>Table 4.1:</b> Summary of Results for fitting performance and Residual analysis of the Linear Regression Models.....	22
<b>Table 4.2:</b> Results of analysis of variance test showing which PMs are dependent on which variables.....	23
<b>Table 4.3:</b> Summary of fitting performance for the artificial neural networks.....	23
<b>Table 4.4:</b> Efficient solutions for the excess machine capacity application.....	29
<b>Table 4.5:</b> Efficient solutions for the dimensional quality and economics critical application.....	33
<b>Table 4.6:</b> Levels of controllable variables used for the dataset for $x,y$ dependent PMs.....	34
<b>Table 4.7:</b> Efficient solutions for the quality critical application.....	40
<b>Table A.1:</b> Initial dataset used to fit metamodels obtained from Moldflow Simulations.....	47

## CHAPTER 1

### INTRODUCTION AND RESEARCH OBJECTIVES

#### 1.1 Introduction:

Injection Molding (IM) is considered the most prominent process for mass-producing plastic parts. More than one third of all plastic products are made by injection molding, and over half of the world's polymer processing equipment is used for the injection molding process [1]. Selecting the proper IM process settings is crucial because the behavior of the polymeric material during shaping is highly influenced by the process variables. Consequently, the process variables govern the quality of the part produced. A substantial amount of research has been directed towards determining the process settings for the IM process as well as the optimal location of the injection gate.

The most widely used approach to determine the process settings is to optimize performance measures as functions of the input variables. This is done by using a model to relate the behavior of the performance measures to the controllable variables and then optimizing these models. Two types of models can be used. The first type is the physics-based model: a model that is based on the physical laws that govern the phenomenon of interest. When the physics of a system are not completely understood or become very complicated, it is more convenient to use the second type of model that is called a metamodel. A metamodel is an empirical expression that is fit to mimic an initial data set that can be obtained from a physics based model or the physical system itself. The

advantage of the metamodel is that once it is created, it can yield large amounts of predictions quite fast. Two types of metamodels were considered in this project: linear regression models, and artificial neural networks. The use of artificial neural networks to model polymer processes is a relatively new area for research.

These metamodels are used to represent the behavior of a single PM as a function of the input variables. It is common practice to optimize these models one at a time. However, difficulties arise when trying to optimize more than one performance measure simultaneously because they often show conflicting behavior. Consider an example of two PMs in IM: part warping and cycle time. Both of these performance measures are greatly affected by the temperature at which the part is ejected. Allowing the part to cool to a lower ejection temperature would favorably decrease the part warping. However, this would also increase the cycle time, which means that fewer parts would be produced. Therefore, to effectively optimize an IM process, a compromise must be found between all the PMs of interest. The problem of considering several PMs simultaneously is referred to as a multiple criteria optimization. Conventional methods of multiple criteria optimization involve assigning weights to the individual performance measures. These methods will converge to a single optimum point, but this solution is dependent on the bias of the user defining the weights. Often times in engineering practice it is impossible to define one optimal solution to all criteria. Instead, it is feasible to determine the best compromises between PMs: that is the combinations of PMs that cannot be improved in one single dimension without harming another. The method used in this project, DEA, provides an unbiased way to find these efficient compromises in a multiple criteria optimization.

This thesis demonstrates a process for finding the best compromises (formally called pareto-efficient solutions, or simply efficient solutions) between several performance measures for one case of IM. Through finding the efficient compromises between PMs, one can trace back the corresponding levels of the controllable variables. The case study presented to illustrate the procedure is based on data obtained by running computer simulations on a “virtual” part shown in **Figure 1.1**. This part represents a case where the location of the weld lines (seam created where two different flow-fronts meet, usually weaker than the rest of the part) is critical and the final part flatness plays a major role. The modeling/optimization procedure demonstrated in this case study is proposed as applicable to more general applications in polymer processing.

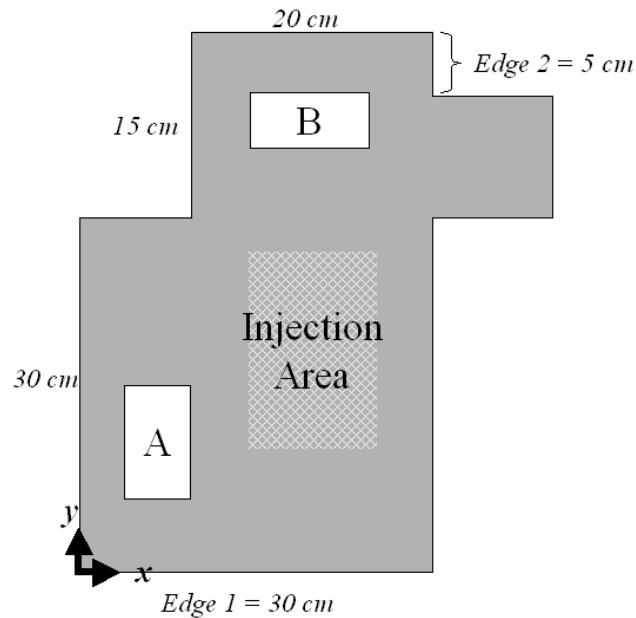


**Figure 1.1:** Schematic of the virtual part with constant thickness and window frame cutouts

## **1.2 Research Objectives:**

- Compare the use of linear regression models and neural networks to represent performance measures of interest in the production of injection molded parts.
- Use Data Envelopment Analysis (DEA) to determine the best compromises between several performance measures in IM applications.
- Determine the best combinations of process variables for an IM process

The primary goal of my thesis is to demonstrate a useful modeling/optimization strategy through an example of one case study of an IM process. I will also investigate the capability of neural networks to model performance measures in the production of injection molded parts. Another essential component of the optimization strategy is the multiple criteria optimization problem, which I will solve through the use of DEA. Finally, using the results of the DEA I will find the best settings for an IM application. I anticipate that the procedure applied in my thesis will prove a useful modeling/optimization procedure that can be applied in practice to IM, and potentially to other polymer processes.

## CHAPTER 2

### METHODOLOGY

#### 2.1 The Optimization Strategy

As proposed by Cabrera-Rios, et al [2, 3] the general strategy to find the best compromises between several PMs is shown in **Figure 2.1**. The optimization strategy consists of five steps:

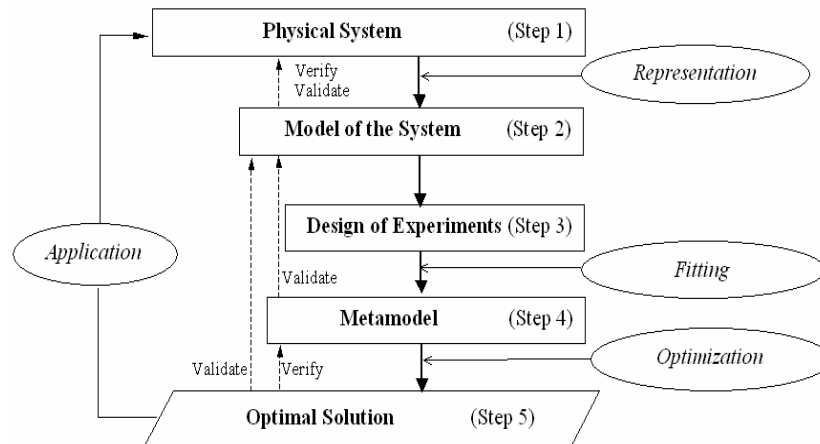


**Figure 2.1:** Schematic of Optimization Strategy

1. **Define the Physical System:** Determine the performance measures, the phenomena of interest, the controllable and non-controllable variables, the experimental region, and the responses that will be included in the study.

2. **Obtain a Model of the System:** Build physics-based models to represent the phenomena of interest in the system. Define models that relate the controllable variables to the responses of interest. If this is not feasible, skip this step
3. **Run Experimental Designs:** Create data sets by either systematically running the models from the previous step, or by performing an actual experiment in the physical system when a mathematical/physics based model is not possible.
4. **Create Metamodels:** Fit metamodels to the results of the experiments. Create empirical expressions (metamodels) to mimic the functionality in the data sets.
5. **Optimize the Physical System:** Use the metamodels to obtain predictions of the phenomena of interest, and to find the best compromises among the PMs for the original system. The best compromises are identified here through DEA.

In the method outlined here, the metamodels are empirical approximations of the functionality between the controllable (independent) variables, and the responses (dependent variables). These metamodels are used either for convenience or from necessity. Because the type of optimization in this work, namely DEA, requires that many response predictions be made, it is more convenient to obtain these predictions from metamodels rather than more complicated physics-based models that may take considerable time to run. In addition, when physics-based models are not available to represent the phenomena of interest, the use of metamodels becomes essential.

## 2.2 Experimental Methodology

For this case study, the interest is the analysis and optimization of the IM process of a particular part shown in **Figure 1.1**. This part represents a case where the location of the weld lines is critical, and the part flatness plays a major role. Weld lines are the seams that occur where two different polymer flow fronts come together. These seams tend to be the structurally weakest area of the part. The part is to be injection molded using a Sumitomo IM machine using PET with a fixed flow rate of 9cc/s. The process and design variables included in this study were the mold temperature,  $T_w$ , the plastic temperature at injection,  $T_m$ , the plastic temperature at ejection,  $T_e$ , the horizontal position of the injection gate,  $x$ , and the vertical position of the injection gate,  $y$ . The injection location was assumed to be constrained to the area shown in **Figure 1.1** due to machine constraints. All of these variables were varied at three levels except for  $T_e$ , which was varied at two levels. Initial results showed that within the feasible range for  $T_e$ , a third level added no meaningful variation. The levels of the process variables are shown in **Table 2.1**.

**Table 2.1:** Levels of the controllable variables used to obtain initial experimental data

$T_m$	$T_w$	$T_e$	$x$	$y$
C	C	C	cm	cm
260	120	149	15	10
275	130	159	20	17.5
290	140		25	25

Nine performance measures were included in this study: the pressure at the injection location,  $P_I$ , the maximum shear stress at the wall,  $S_w$ , the time for the part to cool to the ejection temperature,  $t_f$ , the maximum deflection range in the z-direction,  $R_z$ , the time at which the flow front touches hole A,  $t_A$ , the time at which the flow front

touches hole B,  $t_B$ , the time at which the flow front touches the outer edge of the part,  $t_{oe}$ , the vertical distance from the weld line to edge 1,  $d_1$ , and the horizontal distance from the weld line to edge 2,  $d_2$ . **Figure 2.2** shows how some of these performance measures are obtained.

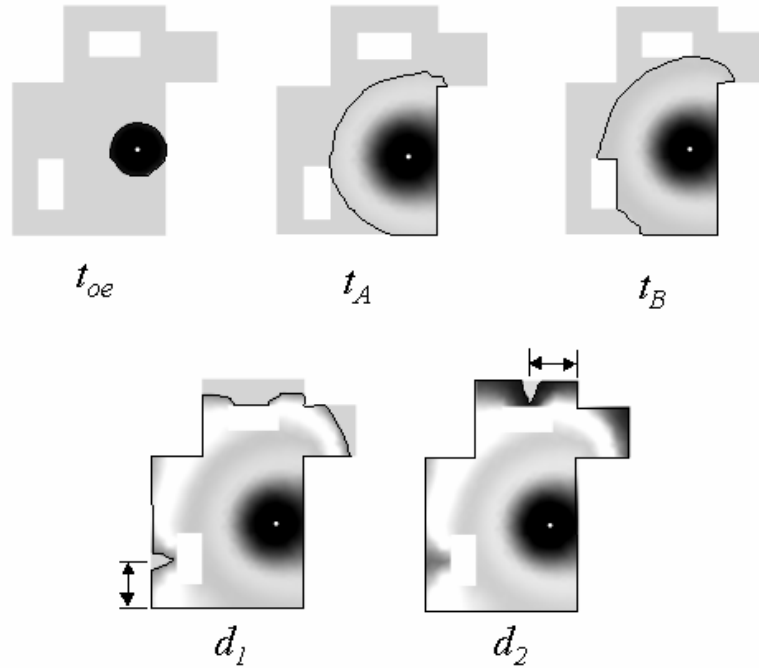


**Figure 2.2:** Schematics to define how  $t_A$ ,  $t_B$ ,  $t_{oe}$ ,  $d_1$ , and  $d_2$  were found.

These particular performance measures were chosen, because they are good indicators of process efficiency (i.e. cycle time) and resulting part quality.  $P_I$  should be minimized to keep the machine capacity unchallenged.  $S_W$  should be minimized as well because large shear stresses can degrade the plastic.  $t_f$  should be minimized in order to reduce the cycle time.  $R_Z$  should be minimized to provide dimensional control (the  $z$  direction was assumed to be the critical dimension).  $T_A$ ,  $t_B$ , and  $t_{oe}$  should all be maximized to reduce potential for flashing (leakage) and provide a balanced flow.

Finally,  $d_1$  and  $d_2$  should be maximized in order to keep the weld lines away from corners we assumed to be subject to large mechanical loading.

Using the different levels of the controllable variables shown in **Table 2.1**, a full factorial Design of Experiments was run using the finite element plastics simulation software *Moldflow*. The constant parameters mentioned previously were also defined in *Moldflow*. A full factorial design implies that every possible combination of the controllable variables was used. The total number of runs for this design was 162. The experimental design was not simplified because it is necessary to have a robust initial dataset from which to create the metamodels. Also, none of the combinations that produced outliers were eliminated. When outliers occurred, the run pertaining to the combination was carefully verified. If an error was detected on the run, the information was corrected, but otherwise it was kept to preserve this information when creating the Metamodels. A validation set was also created using different levels of the controllable variables in order to test the prediction capabilities of the metamodels. The controllable variable levels used for the validation set are shown in **Table 2.2**.

**Table 2.2:** Levels of the controllable variables for the validation dataset

$T_w$	$T_m$	$T_e$	$x$	$y$
$C$	$C$	$C$	$cm$	$cm$
125	267.5	154	17.5	13.75
135	282.5		22.5	21.25

Two types of metamodels were considered: linear regression models and artificial neural networks. The linear regression models were generated using the computer software *MINITAB*. The same software was used to conduct a statistical analysis of

variance. The statistical analysis was used to pinpoint which of the controllable variables significantly affected each of the performance measures. The neural networks were created using the *Neural Network Toolbox* in *MATLAB*. The metamodels were trained from the initial dataset resulting from the 162 simulations run in *Moldflow*.

To solve the optimization problem, it was necessary to generate a large number of feasible level combinations of the controllable variables. This was achieved by varying  $T_m$  and  $T_w$  at five levels, and the rest of the variables at three levels within the experimental region of interest in a full factorial enumeration, which resulted in a total of 675 combinations. The decision on the levels for each variable was made considering the feasible resolution in a real IM machine. Using a resolution of 0.5 °C for mold temperature has no meaning due to the high variability of this variable. The levels of the controllable variables used for this dataset are shown in **Table 2.3**.

**Table 2.3:** Levels of the controllable variables for the dataset that was the subject of the Multiple Criteria Optimization

$T_m$	$T_w$	$T_e$	$x$	$y$
C	C	C	cm	cm
260	120	149	15	10
267.5	125	154	20	17.5
275	130	159	25	25
282.5	135			
290	140			

## CHAPTER 3

### TECHNICAL BACKGROUND

#### 3.1 Injection Molding:

IM is considered the most important manufacturing process for mass producing plastic parts. Over one half of all polymer-processing equipment is used for injection molding, and over a third of all thermoplastic parts are manufactured by IM [1]. The most common type of injection molding machine is called a reciprocating screw machine. A schematic of a typical injection molding machine is shown in **Figure 3.1**.

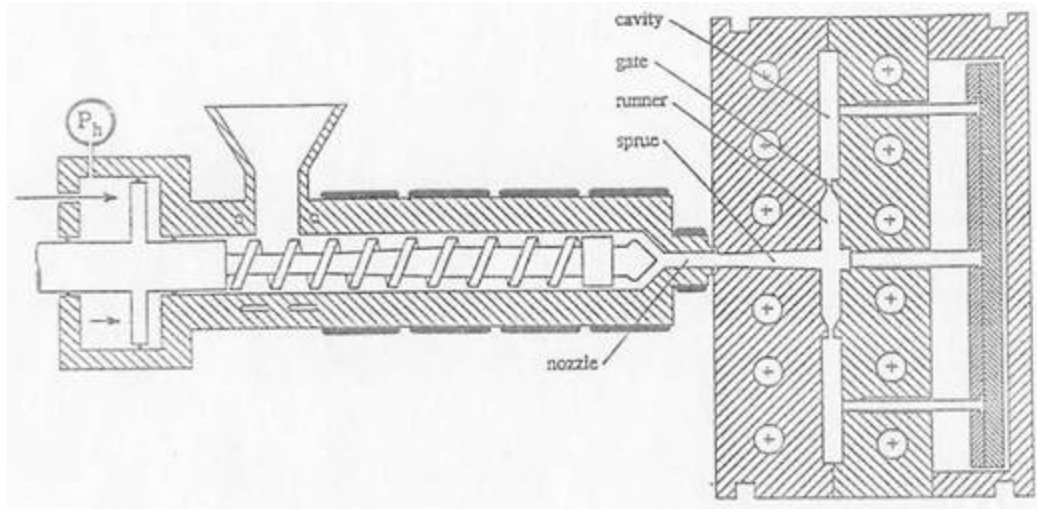


**Figure 3.1:** Typical reciprocating screw injection molding machine [4]

Before the actual injection molding cycle begins, the material is fed in to the hopper in the form of pellets. Due to the shear heating between pellets and the heaters

placed around the barrel, the pellets are melted. The injection molding cycle begins with the screw turning in order to accumulate the plastic at the front of the barrel. As the plastic is accumulating at the front of the barrel, the screw is forced backwards. When the proper amount of plastic is accumulated, the screw plunges forward and injects the plastic into the mold cavity. After the cavity is filled, the machine increases the pressure to the holding pressure. Once the material cools to the defined ejection temperature, the mold opens, and the part is ejected. The cycle is then repeated.

A graph of the pressure at the point of injection is shown in **Figure 3.2**. During the injection of the plastic, the pressure increases. Once the plastic is injected, the machine ramps the pressure up to a holding pressure defined by the user. This high pressure phase is used to counteract the effects of material shrinkage due to the cooling of the part. The holding phase ends either when the gate freezes (cold runner) or by closing a valve when the user desires (hot runner).

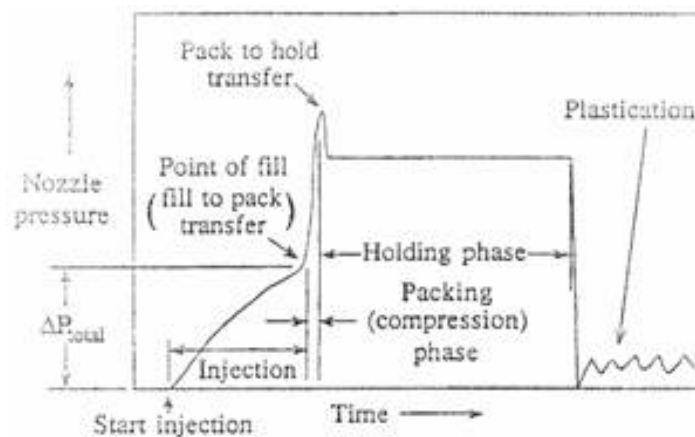


**Figure 3.2:** Pressure at the injection location for one cycle of injection molding [4]

### 3.2 Metamodeling:

Metamodels were used in order to obtain relationships that related the controllable variables to the performance measures of interest. A metamodel is an empirical expression that approximates the functionality between the performance measures and the input variables. The data obtained from the experimental design described in the previous section was used to train the metamodels. A secondary validation dataset that was not used to fit the metamodels was employed to test the prediction capabilities of the metamodels. Two types of metamodels were investigated: linear regression models and artificial neural networks.

#### 3.2.1 Linear Regression Models:

The general form of a linear regression model is defined as follows:

$$y = \mathbf{b}_0 + \mathbf{b}_1 x_1 + \mathbf{b}_2 x_2 + \dots + \mathbf{b}_n x_n + \mathbf{e} \quad (3.1)$$

The parameters  $\mathbf{b}_i$  ( $i=0, 1, 2, \dots, n$ ) are called the regression coefficients.  $\mathbf{b}_i$  describes the expected change in output  $y$  per unit change in input  $x_i$  when all of the other input variables are held constant [5]. A regression model can contain higher order terms. Any form of this equation that is linear with respect to the regression coefficients is referred to as a linear regression. The goal of a linear regression model is to determine the regression coefficients that minimize the sum of the squared errors between the regression model output, and the PM data that it is intended to represent. This is accomplished by the least squares method.

For this study a second order regression model was used. The equation for this model is:

$$y = \mathbf{b}_0 + \sum_{i=1}^N \mathbf{b}_i x_i + \sum_{i=1}^{N-1} \sum_{j>i}^N \mathbf{b}_{ij} x_i x_j + \sum_{i=1}^N \mathbf{b}_{ii} x_i^2 \quad (3.2)$$

where N is the total number of independent variables. When using linear regression one must verify, besides the goodness of the fit conventionally measured by the  $R^2$  value, that the basic assumptions of the model have been met. This is done by means of the analysis of residuals to make sure that these are normally and independently distributed with mean 0 and constant but unknown variance  $\mathbf{s}^2$  [6]. A second method that was used to evaluate the prediction capabilities of the metamodels was the mean absolute prediction error (MAPE). It was calculated using the following equation:

$$MAPE = \frac{100}{N} \sum_{i=1}^N \left| \frac{y_i - \hat{y}_i}{y_i} \right| \quad (3.3)$$

where N is the total number of experimental points and  $y_i$  and  $\hat{y}_i$  are experimental response and the predicted response at the  $i^{th}$  experimental point respectively [8].

### 3.2.2 Artificial Neural Networks:

The second type of metamodel that was evaluated is called an artificial neural network (ANN). An ANN is an information processing system that behaves similarly to a biological neural network. It is made up of processing units called neurons that are classified into three layers: input layer, hidden layer, and output layer. Each of these neurons applies an activation function to the net input signal. Information is transferred from one neuron to another by connection links. Each connection link applies an associated multiplier, called a weight. A bias, another weight, is added to the sum of all

products pertaining to the incoming links [7]. A schematic of a simple ANN with three inputs, two hidden neurons, and two outputs is shown in **Figure 3.3**.

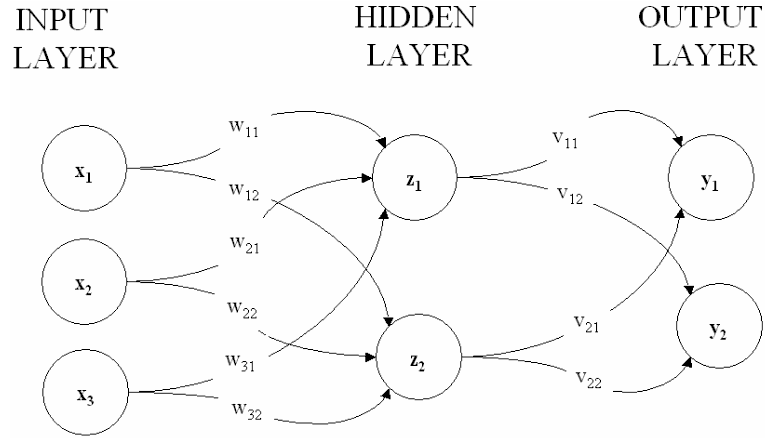


**Figure 3.3:** Schematic of an artificial neural network with three inputs, two neurons in the hidden layer, and two outputs

ANNs are characterized by three things: its pattern of connections between neurons, its algorithm for determining the weights and biases, and the activation functions applied at the individual neurons. The neural networks used in this application will have one input layer with  $k$  inputs (independent variables), one hidden layer with  $m$  neurons (hidden neurons), and one output layer with  $n$  neurons (dependent variables). The input layer and output layer will apply linear activation functions, and the hidden layer will apply a tangent sigmoid activation function. The basic functional form of the artificial neural network described here is given by:

$$Y = \Phi(W_2^T \Psi(W_1 P + b_1) + b_2) \quad (3.4)$$

where  $P$  is a vector of length  $k$  containing the independent variables.  $W_1$  and  $W_2$  are matrices that contain the weights to be applied on connection links between the input and hidden layers and between the hidden and output layers respectively.  $b_1$  and  $b_2$  are vectors containing the biases that are added at connection links between the input and hidden layers and between the hidden and output layers respectively [7].

There are several algorithms that can be used to determine the weights and biases for the network. In this application, a back propagation algorithm was chosen. This algorithm implies an iterative process. The error of the neural networks is measured by the sum of the squared errors between the prediction and the experimental data. The weights and biases are changed incrementally after each iteration. The neural network will continue cycling through the functional form of equation 3.4 until it either finds a minimum to the error function or reaches a user-defined maximum number of iterations. It is possible that the neural network will converge to a local minimum in the error. Therefore, it is necessary to train the data several times starting from different values of weights in order to increase the chance that a global minimum is found [5].

In general, ANNs are very effective for modeling highly nonlinear data. The number of neurons applied in the hidden layer along with the values of the weights determines the complexity of the network output. When fitting the ANNs initially one neuron was used in the hidden layer (hidden neuron). The number of hidden neurons was increased until the network output was able to fit the training data well and still make good predictions for the validation data. If the number of neurons in the hidden layer is increased indefinitely, it is likely that the output of the neural network would pass exactly through the training data. However, at some point, the behavior of the neural network

becomes much more complicated than is reasonable for the PM in the physical system, and the network loses the capacity to make predictions for points in between the training datapoints. This is referred to as over fitting. In this application, while the validation set was not used to fit the neural networks, the error between the ANN output and the validation set was simultaneously considered as the network was trained. The training was stopped early when this error began to deteriorate in order to avoid overfitting. Without stopping the training early, it is possible that error for the training data would have improved, but the ANN would have lost some of its prediction capability.

### **3.3 Data Envelopment Analysis:**

Once the metamodels were obtained, they were used to generate a large dataset which then became the subject of a multiple criteria optimization. The method used in this research to solve the multiple criteria optimization problem is called Data Envelopment Analysis. The goal of data envelopment analysis is to determine the data points which dominate the rest of the dataset. These are the points that cannot be improved with respect to any one PM without harming another. The combination of these points makes up the efficient frontier. The number of PMs considered determines the dimensionality of a multiple criteria optimization problem. The efficient frontier can only be visualized in two or three dimensions. The efficient frontier found by DEA of a sample dataset with two PMs is shown in **Figure 3.4**.

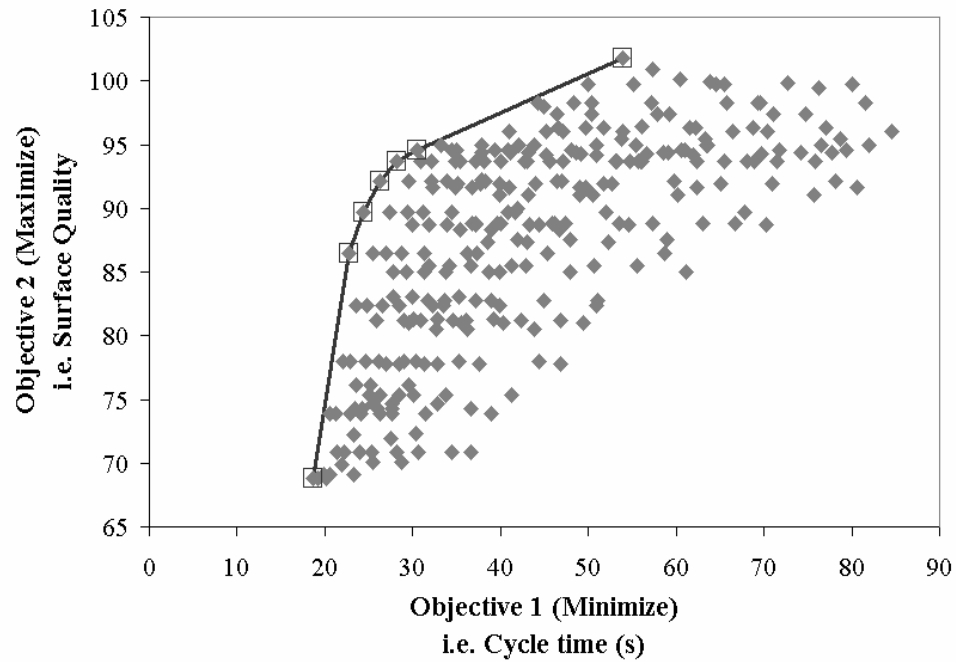


**Figure 3.4:** Sample dataset with the efficient frontier found by DEA shown

In this case we want to minimize the PM on the  $x$  axis (move to the left) and maximize the PM on the  $y$  axis (move to the top). In general, it is desirable to move towards the top left region of the dataset. In this two-dimensional case, it is easy to visualize the envelope that the efficient frontier forms over the dataset, hence the name Data Envelopment Analysis.

Cabrera-Rios et al [2,3] have demonstrated the use of DEA to solve multiple criteria optimization problems in polymer processing. DEA, a technique created by Charnes, Cooper, and Rhodes [12], provides a way to measure the efficiency of a given combination of PMs relative to a finite set of combinations of the same PMs. The efficiency of each combination is computed through the use of two linearized versions of the following mathematical programming problem in ratio form:

$$\text{Find } \theta, \mu, m_0 \text{ to}$$

$$\text{Maximize } \frac{\mu^T \mathbf{Y}_0^{\max} + m_0}{\theta^T \mathbf{Y}_0^{\min}} \quad (3.5.1)$$

s.t.

$$\frac{\mu^T \mathbf{Y}_j^{\max} + m_0}{\theta^T \mathbf{Y}_j^{\min}} \leq 1 \quad j = 1, \dots, n \quad (3.5.2)$$

$$\frac{\mu^T}{\theta^T \mathbf{Y}_0^{\min}} \geq \mathbf{e} \cdot \mathbf{1} \quad (3.5.3)$$

$$\frac{\theta^T}{\theta^T \mathbf{Y}_0^{\min}} \geq \mathbf{e} \cdot \mathbf{1} \quad (3.5.4)$$

$$m_0 \text{ free} \quad (3.5.5)$$

where,  $\mathbf{Y}_0^{\max}$  and  $\mathbf{Y}_0^{\min}$  are vectors containing the values of those PMs of interest to be maximized and minimized respectively,  $\mathbf{m}$  is a vector of multipliers for the PMs to be maximized,  $\mathbf{n}$  is a vector of multipliers for the PMs to be minimized,  $m_0$  is a scalar variable,  $n$  is the number of total combinations in the set, and  $\mathbf{e}$  is a very small constant usually set to a value of  $1 \times 10^{-6}$ .

In order to avoid an infinite number of solutions in ratio form, linearization is necessary [10]. Linearization is achieved by setting the denominator of Eq. 3.5.1 to a value of 1, while multiplying both sides of Eq. 3.5.2 by the denominator of its left-hand-side; the inequalities in Eqs. 3.5.3 and 3.5.4 are simplified once the denominator takes the value of 1; and Eq. 3.5.5, can be decomposed into the difference of two nonnegative variables. The constraints of Eqs. 3.5.3 and 3.5.4 are imposed to keep the multipliers from going to zero. Following these manipulations, one obtains the first linear version of the problem, called the input-oriented model [10]. The second linearization is obtained by inverting the ratios in the original formulation (Eqs. 1 through 5) and keeping the variable  $m_0$  in the numerator in Equations 3.5.1 and 3.5.2. The rest of the linearization

steps are similar to those described before. This second linearization is called the output-oriented model and it is a minimization problem.

The efficiency score obtained from solving the input-oriented model for each combination ranges from 0 to 1 and is relative to all  $n$  combinations. Those combinations with efficiency of 1 are deemed efficient. The output-oriented model yields efficiencies that range from 1 to infinity, with 1 being the perfect efficiency score. A particular combination will be considered efficient when both the input-oriented and the output-oriented models identify it as efficient. The collection of efficient combinations makes up the (piece-wise) efficient frontier of the entire set. These efficient combinations dominate any other combination not on the frontier. In other words, at the efficient frontier, no single PM can be improved without harming another one [6].

## CHAPTER 4

### RESULTS

#### 4.1 Metamodeling Results:

In general, it is desirable to fit a simple model to the data. In this study, linear regressions were initially considered as models for the performance measures. When simple models do not suffice, then more complicated models, in this case ANNs, become necessary. In general the tradeoff that exists between the linear regression models and the ANNs is that the ANNs are more difficult and time-consuming to create, but they are much more suitable for modeling highly nonlinear data.

The results of the fitting performance of the regression metamodels obtained for each of the nine PMs are presented on **Table 4.1**. The performance is described by the  $R^2$  value, as well as the mean absolute percent prediction error (MAPE), which was described earlier. Also reported in **Table 4.1** is the MAPE for the validation data set. This second MAPE is useful to understand the prediction capabilities of the metamodel. An analysis of residuals showed that in one case, the data violated two of the basic assumptions of the linear regression models: normal distribution and a constant variance.

**Table 4.1:** Summary of Results for fitting performance and Residual analysis of the Linear Regression Models

		$P_I$	$S_W$	$t_f$	$R_Z$	$t_A$	$t_B$	$t_{oe}$	$d_1$	$d_2$
Performance	$R^2$ (%)	96.6	98.98	99.45	96.17	99.34	99.57	78.29	85.98	97.4
	MAPE (%)	3.63	1.3	1.71	27.96	5.65	2.84	33.27	23.64	4.06
	MAPE Validation (%)	8.632	7.681	2.031	15.29	10.87	4.325	30.31	16.31	6.766
Residual	Normality	Yes	No	Yes						
	Independence	Yes	Yes	Yes						
	Constant Variance	Yes	No	Yes						

The statistical tests for the significance of each of the coefficients of the regression metamodels led to the results shown in **Table 4.3**. The boxes shaded in gray show which components of the regression model significantly affected each PM. Notice that several PMs are only dependent on the design variables  $x$  and  $y$  ( $t_A$ ,  $t_B$ ,  $t_{oe}$ ,  $d_1$ ,  $d_2$ ). This means that for each  $x,y$  pair, the result for these PMs will be the same regardless of the levels of the temperatures. This analysis of variance gave us critical knowledge to simplify and extract meaning from the solution of the multiple criteria optimization which is discussed later [9].

**Table 4.2:** Results of analysis of variance test showing which PMs are dependent on which variables

		Performance Measures								
		$P_I$	$t_f$	$S_W$	$R_Z$	$t_A$	$t_B$	$t_{oe}$	$d_1$	$d_2$
Linear Terms	$T_w$									
	$T_m$									
	$T_e$									
	$x$									
	$y$									
Quadratic Terms	$T_w^2$									
	$T_m^2$									
	$T_e^2$									
	$x^2$									
	$y^2$									
Second Order Interactions	$T_w T_m$									
	$T_w T_e$									
	$T_w x$									
	$T_w y$									
	$T_m T_e$									
	$T_m x$									
	$T_m y$									
	$T_e x$									
	$T_e y$									
	$xy$									

Because DEA as we applied it in this research relies heavily in the prediction of PMs at a large amount of untried combinations of controllable variables, it is worthwhile to try to fit metamodels that allow us to obtain closer predictions within the experimental region of interest. With this in mind, it was decided to consider a more complicated model, namely ANNs. The fitting performance of the ANNs is presented **Table 4.3**.

**Table 4.3:** Summary of the fitting performance for the artificial neural networks

		$P_I$	$S_W$	$t_f$	$R_Z$	$t_A$	$t_B$	$t_{oe}$	$d_1$	$d_2$
Performance	$R^2$ (%)	99.98	97.89	99.99	99.1	100	99.98	100	97.04	99.43
	MAPE (%)	0.2	2.02	0.21	8.6	0.25	0.43	0.36	7.26	1.29
	MAPE Validation (%)	3.66	5.76	0.24	6.68	3.66	2.42	6.17	4.87	1.38

It is worth mentioning that when fitting the ANNs, it was an explicit goal to achieve better prediction capability than that obtained through linear regression. This was achieved by allowing the training of the neural networks to stop at the point where the prediction error started to deteriorate. The results are evident when comparing the MAPE values for the validation set in **Tables 4.1** and **4.3**. The prediction capabilities of the ANNs outperformed those of the linear regression models. For this reason the ANNs were used to create the dataset needed for the use of DEA [9].

#### **4.2 Data envelopment Analysis Results:**

The complete multiple criteria optimization problem originally posed for this case contained all nine performance measures. To solve the optimization problem, it was necessary to generate a large number of feasible level combinations of the controllable variables. This was achieved by varying the controllable variables at the levels shown in **Table 2.2** in a full factorial enumeration totaling 675 combinations. The number of levels for these variables was decided based on how accurately we could control them in a real IM machine. The results after applying DEA to the full set of PMs were that over 400 of the 675 combinations were found to be efficient. Such a large number of efficient combinations can be explained by examining **Table 4.2**, which summarizes the results of the analysis of variance of each PM in regression form.

Notice that the last five PMs are only dependent on the injection point position determined by variables  $x$  and  $y$ . Any specific combination of values  $(x,y)$  will give the same result on all of these five PMs regardless of the values that the rest of the controllable variables  $T_m$ ,  $T_w$ , and  $T_e$  take. Having used a full factorial enumeration with  $x$

and  $y$  at three levels, it follows that we can obtain only nine different values for these five PMs, but each of the nine specific combinations  $(x,y)$  have in fact 75 combinations of the rest of the controllable variables. Due to the high dimensionality of the problem, this elevated amount of repetition results in a large number of efficient solutions. In order to increase the discrimination power i.e. obtain fewer efficient solutions, one can solve the DEA model shown in Eqs. 1 through 5 by setting  $m_j$  equal to zero. The resulting model is similar to the Charnes-Cooper-Rhodes (CCR) DEA model [10].

Using the simple modification described above, the number of efficient combinations comes down to 149. It can be shown that these combinations are a subset of those 400 plus found previously. These efficient combinations are shown in terms of the PMs in **Figure 4.1**.

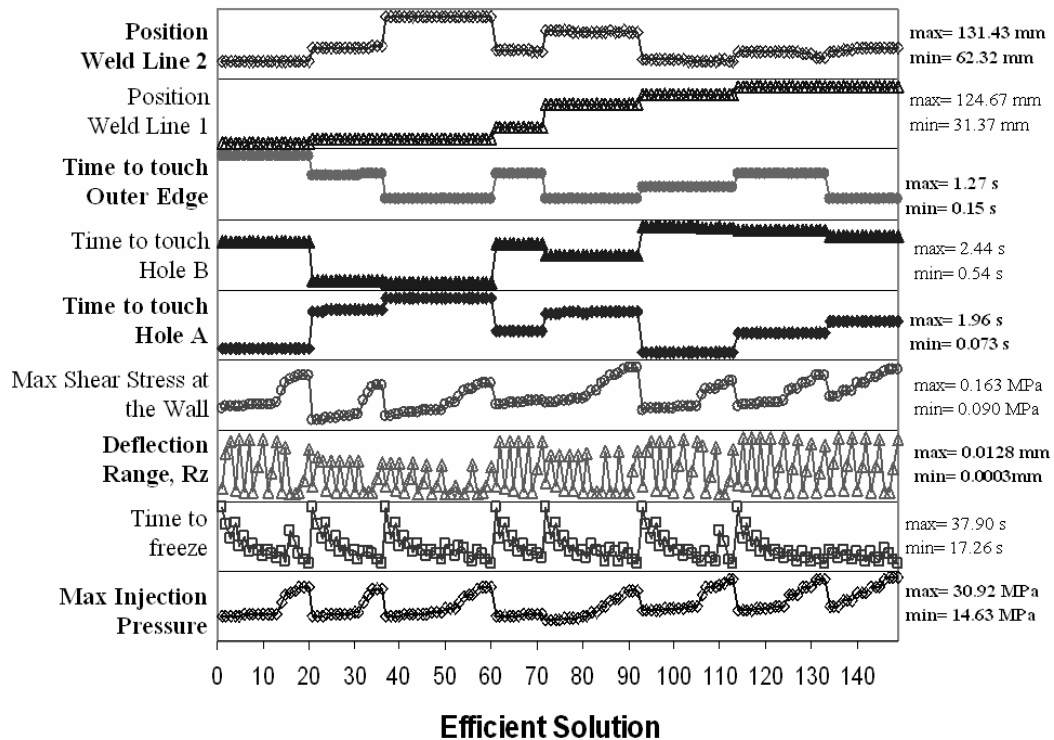


**Figure 4.1:** Levels of the PMs that corresponded to the efficient solutions when all nine were included

It is important to notice that we can exploit the information our methods gave us about the functionality of our PMs in order to tailor our optimization problem. To illustrate, five sub cases were defined for practical applications of the conceptual part shown in **Figure 1.1**: (i) a excess capacity injection machine application, (ii) a dimensional quality and economics critical application, (iii) a structural part application, (iv) a quality critical application, (v) and a case including PMs that are only dependent on the injection location [11].

*Excess Capacity Injection Molding Machine:*

For a case in which the injection-molding machine has excess capacity, it would be possible to not consider the maximum injection pressure in the optimization problem. For simplicity, in this case  $S_W$ ,  $t_A$ ,  $t_B$ , and  $t_{oe}$  were also dropped from the optimization, leaving four performance measures. The DEA model was again solved here by setting the constant  $m_0$  equal to zero in order to improve the discrimination power of DEA. The functionality shown in **Table 4.1** called for inclusion of all variables, and so we used the factorial enumeration with 675 combinations. In this case, fourteen combinations were found to be efficient. **Figure 4.2** shows the levels of the PMs for the efficient solutions. The compromise between the locations of the weld lines is evident. A noticeable compromise also arises between  $t_f$  and  $R_z$ . This is an understandable compromise, because the two depend oppositely on the ejection temperature.

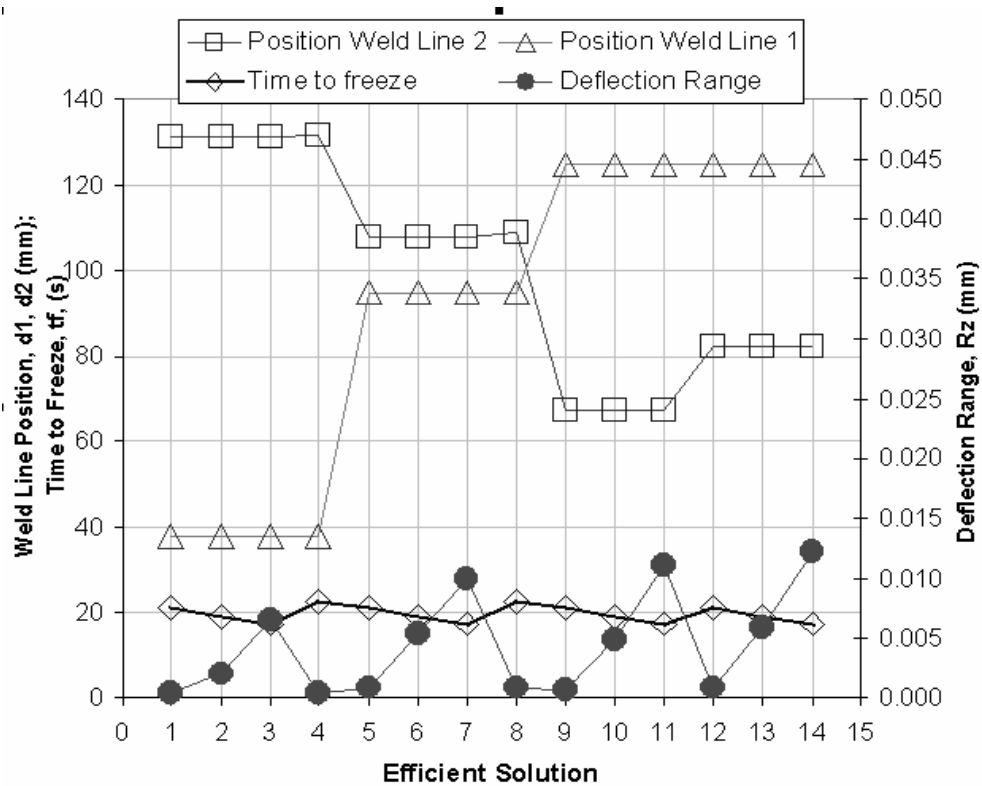


**Figure 4.2:** Efficient solutions for the excess machine capacity application in terms of the levels of the PMs considered.

**Figure 4.3** shows the locations of the injection gate for the efficient solution. The positions in this case help to define ‘attractive’ areas to locate the injection port, since they tend to cluster in specific sections. In this case the efficient injection locations clustered along right and bottom edges. The three PMs that are affected by the location of the injection gate are the weld line positions and the deflection in the z-direction. The additional PM here is the time to freeze which is not affected by the injection location according to the analysis of variance.

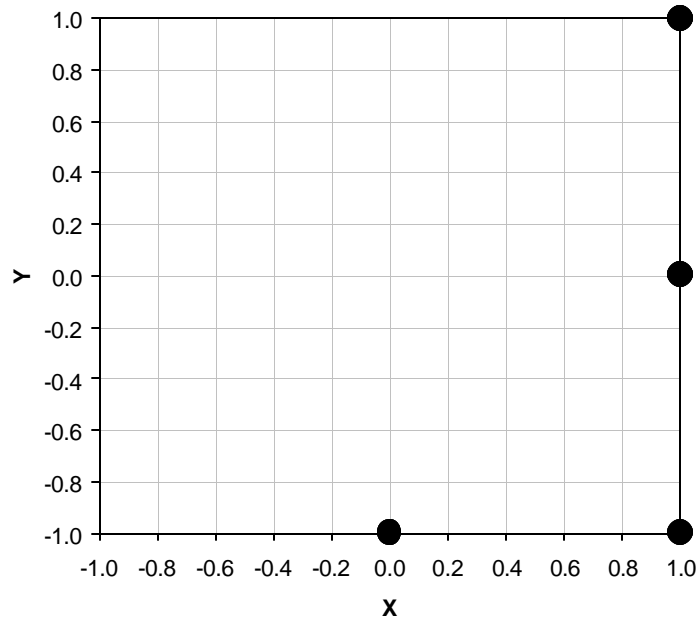


**Figure 4.3:** Injection Locations of the efficient solutions to the excess machine capacity application transformed to fall between -1 and 1.

**Table 4.4** shows the values for all of the controllable variables at the efficient solutions. Notice that  $T_w$  and  $T_m$  were at 120 and 260 degrees Celsius respectively for all of the efficient solutions. In industrial practice, if the PMs involved in this case were the only ones of interest, this would be a good indication that  $T_m$  and  $T_w$  should be set at these temperatures. Also notice that the ejection temperature values of the efficient solutions vary over the entire range. According to the analysis of variance,  $d_1$  and  $d_2$  do not depend on the ejection temperature, so this fact must be due to the compromise between  $R_z$  and  $t_f$  previously mentioned.

**Table 4.4:** Efficient Solutions for the excess machine capacity application

Controllable Variables					Performance Measures			
$x$	$y$	$T_w$	$T_m$	$T_e$	$t_f$	$R_z$	$d_1$	$d_2$
<i>cm</i>	<i>cm</i>	<i>C</i>	<i>C</i>	<i>C</i>	<i>s</i>	<i>mm</i>	<i>mm</i>	<i>mm</i>
25	25	120	260	149	20.89	0.0005	37.9	130.9
25	25	120	260	154	18.99	0.002	37.9	130.9
25	25	120	260	159	17.27	0.007	37.9	130.9
25	25	120	260	149	22.71	0.000	37.9	131.4
25	17.5	120	260	149	20.90	0.001	94.9	107.8
25	17.5	120	260	154	19.00	0.005	94.9	107.8
25	17.5	120	260	159	17.28	0.010	94.9	107.8
25	17.5	120	260	149	22.72	0.001	94.9	108.9
15	10	120	260	149	20.92	0.001	124.6	67.4
15	10	120	260	154	19.02	0.005	124.6	67.4
15	10	120	260	159	17.30	0.011	124.6	67.4
25	10	120	260	149	20.92	0.001	124.7	82.1
25	10	120	260	154	19.02	0.006	124.7	82.1
25	10	120	260	159	17.30	0.012	124.7	82.1

*Dimensional Quality and Economics Critical Application:*

In this case it was assumed that the economic concerns included minimizing the cycle time and keeping the machine capacity untested in order to have long machine life and smaller power consumption. These two concerns are defined by  $t_f$  and  $P_I$  respectively.  $R_z$  defines the dimensional quality. The analysis of variance shows that all of the controllable variables affect at least one of these PMs, so the enumeration with 675 combinations again was applied. Twenty-five efficient solutions were found. Since the problem is three-dimensional the efficient frontier can be visualized. The efficient points are shown in **Figure 4.4** with respect to the rest of the data set.

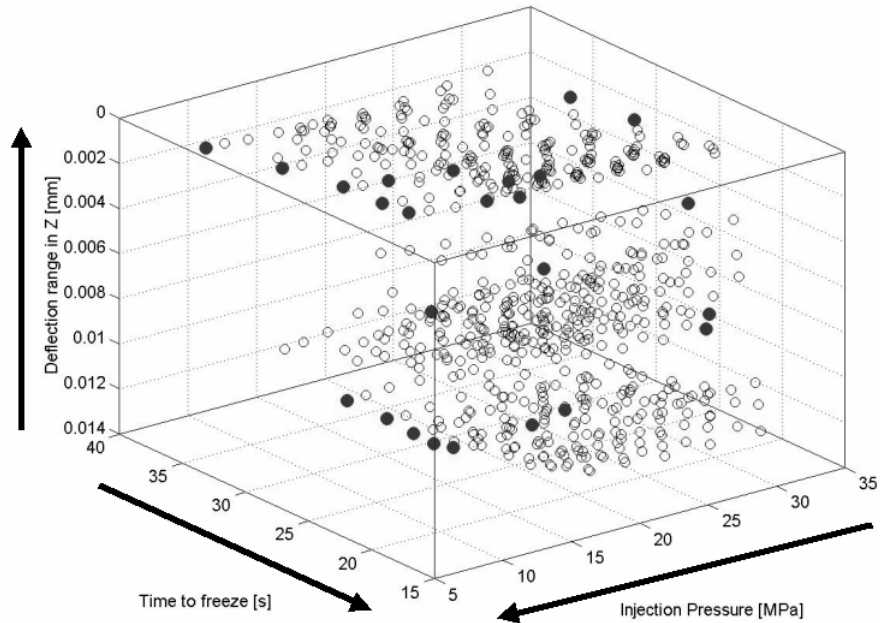


**Figure 4.4:** A Visualization of the efficient frontier of the economics critical and dimensional Application

**Figure 4.5** shows the efficient solutions in terms of the levels of the PMs. The direct compromise between the time to freeze and deflection is confirmed here. Notice that they follow opposite trends and we are trying to minimize both.

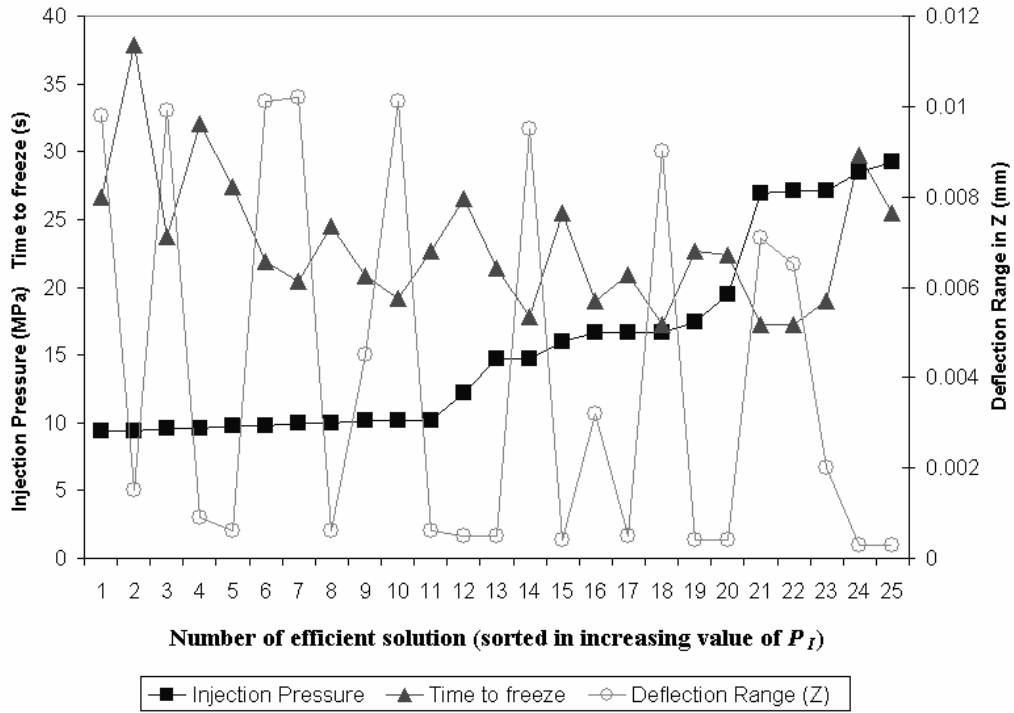


**Figure 4.5 :** Efficient solutions for the dimensional quality and economic application in terms of the levels of the PMs considered.

**Figure 4.6** shows the locations of the injection gate for the efficient solutions. This case contradicts the first case. In the large machine capacity case, the ‘attractive’ areas for the injection gate were found at the bottom and right edges of the feasible area, but in this case, the top edge and bottom left corner proved to be the efficient locations. This is due to the fact that the positions of the weld lines were not considered in this case. From these results we can conclude that  $d_1$  and  $d_2$  are the main drivers for keeping the injection location on the right or bottom edge. They are the only PMs affected by  $x$  and  $y$  that were included in the first case and not in this case.

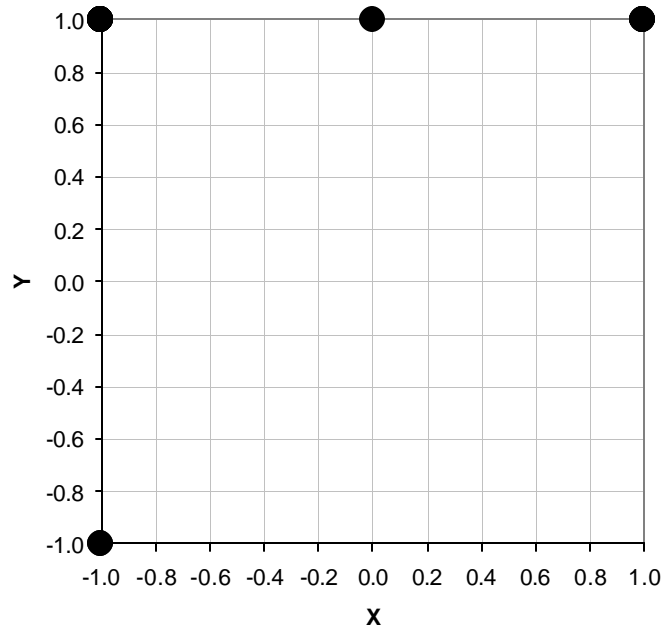


**Figure 4.6:** Injection Locations of the efficient solutions to the dimensional quality and economics critical application transformed to fall between -1 and 1.

**Table 4.5** shows the twenty-five combinations of the controllable variables that proved to be efficient for the dimensional quality and economics critical application. Eighteen out of the twenty-five efficient solutions had the injection gate located at the upper left corner of the feasible region, which is close to the center of the part. This is the most robust injection location for this application. According to the analysis of variance,  $P_I$  is affected by the location of the injection gate. Locating the injection gate towards the center would favorably decrease  $P_i$ . Since  $d_1$  and  $d_2$  were not included in this case there were no negative effects of moving the injection gate towards the center.

**Table 4.5:** Efficient Solutions for the dimensional quality and economics critical application

Controllable Variables					Performance Measures		
$x$	$y$	$T_w$	$T_m$	$T_e$	$P_I$	$t_f$	$R_z$
<i>cm</i>	<i>cm</i>	<i>C</i>	<i>C</i>	<i>C</i>	<i>MPa</i>	<i>s</i>	<i>mm</i>
15	25	140	290	159	9.35	26.7	0.0098
15	25	140	290	149	9.35	37.9	0.0015
15	25	140	282.5	159	9.55	23.8	0.0099
15	25	140	282.5	149	9.55	32.0	0.0009
15	25	140	275	149	9.75	27.4	0.0006
15	25	140	275	159	9.75	21.9	0.0101
15	25	140	267.5	159	9.96	20.4	0.0102
15	25	140	267.5	149	9.96	24.5	0.0006
15	25	140	260	154	10.17	20.9	0.0045
15	25	140	260	159	10.17	19.1	0.0101
15	25	140	260	149	10.17	22.7	0.0006
15	25	130	275	149	12.25	26.5	0.0005
15	25	125	260	149	14.69	21.4	0.0005
15	25	125	260	159	14.69	17.8	0.0095
15	25	120	275	149	16.00	25.5	0.0004
15	25	120	260	154	16.61	19.0	0.0032
15	25	120	260	149	16.61	20.9	0.0005
15	25	120	260	159	16.61	17.3	0.0090
25	25	140	260	149	17.46	22.7	0.0004
25	25	135	260	149	19.43	22.4	0.0004
20	25	120	260	159	26.92	17.3	0.0071
25	25	120	260	159	27.16	17.3	0.0065
25	25	120	260	154	27.16	19.0	0.0020
15	10	120	282.5	149	28.50	29.8	0.0003
15	10	120	275	149	29.21	25.5	0.0003

### *A Structural Application*

In this application, the PMs included were the vertical distance from edge 1 to the weld line,  $d_1$ , and the horizontal distance from edge 2 to the weld line,  $d_2$ . The location of weld lines is considered critical to design a structurally sound part. From the analysis of variance, it was known that these PMs depended only on the position of the injection gate, characterized by variables  $x$  and  $y$ . In order to avoid the repetition described in the

full set, a new dataset was created by varying  $x$  and  $y$  at nine levels creating a finer sampling grid for the injection location. The rest of the variables were set to a value in the middle of their respective ranges. The levels of the controllable variables for this dataset are shown in **Table 4.6**. The total number of combinations of controllable variables in this dataset was 81.

$T_m$	$T_w$	$T_e$	$x$	$y$
$C$	$C$	$C$	$cm$	$cm$
130	275	154	15	10
			16.25	11.875
			17.5	13.75
			18.75	15.625
			20	17.5
			21.25	19.375
			22.5	21.25
			23.75	23.125
			25	25

**Table 4.6:** Levels of controllable variables used for the dataset for  $x,y$  dependent PMs

In this two-dimensional case, the efficient frontier is shown here in **Figure 4.7**.

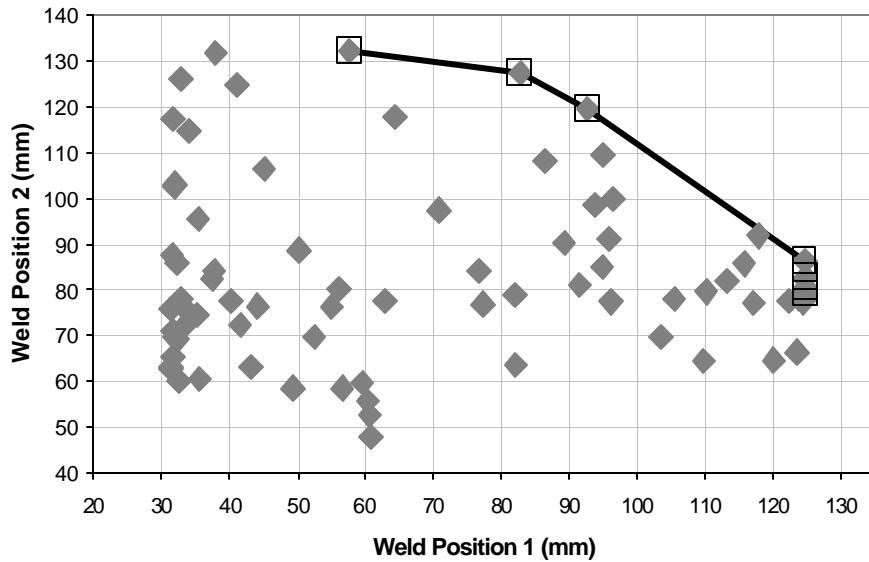


**Figure 4.7:** Visualization of the efficient frontier in the structural application

The seven efficient solutions for a structural part are shown in **Figure 4.8** in terms of the levels of the two PMs in increasing order of  $d_1$ . The compromise between the positions of the weld lines is confirmed. We want to maximize both of the weld line positions, but where one of them is at a maximum, the other is at a minimum.

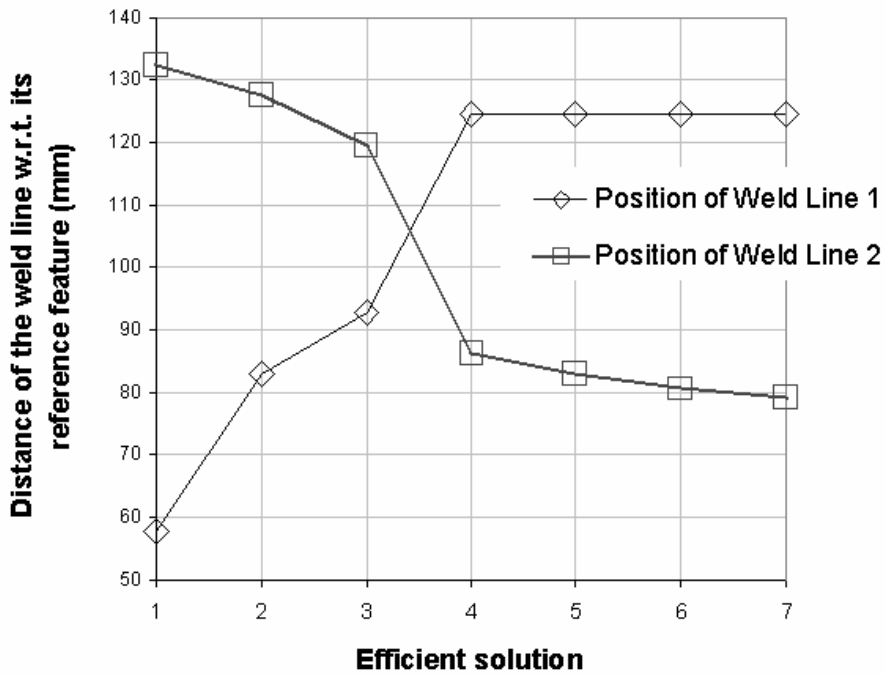


**Figure 4.8:** Efficient Solutions for the structural application in terms of the weld line positions  $d_1$  and  $d_2$ .

**Figure 4.9** shows the positions of the injection gate corresponding to the seven best compromises. The entire area shown is the feasible injection region. In this case the ‘attractive’ clusters occur at the bottom right corner of the feasible injection area and along the right edge of the feasible injection region. These results tend to agree with the large machine capacity case. Since the locations of the weld lines are independent of the other controllable variables, any of these  $x,y$  pairs would obtain the same results for  $d_1$

and  $d_2$  regardless of the temperature levels. In this case the efficient solutions are defined by the injection location, so temperature levels are not shown. In other words, had the temperatures been left at the maximum or minimum of their respective feasible ranges, we would have arrived at the same results for the locations of the weld lines.

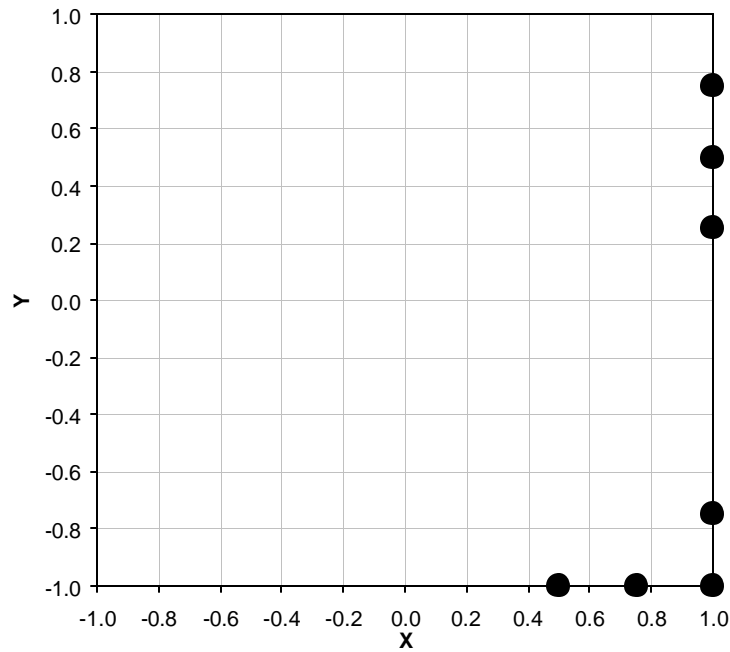


**Figure 4.9:** Injection Locations of the seven efficient solutions to the structural application transformed to fall between -1 and 1.

### *A Quality Critical Application*

Appearance in our test part we defined as related to the position of the weld lines and the flatness of the part, i.e.  $d_1$ ,  $d_2$ , and  $R_Z$ . From the analysis of variance in **Table 4.1** it is known that  $d_1$  and  $d_2$  depend only on the  $x$  and  $y$  position of the injection gate. However, the temperatures cannot be disregarded in this case, because  $R_Z$  depends on all

three of them. Therefore, we used the factorial enumeration already created for all the variables ( $x$ ,  $y$ ,  $T_m$ ,  $T_w$ , and  $T_e$ ) with 675 combinations. The resulting sixteen efficient solutions are shown in **Figure 4.10** with respect to the rest of the dataset. Notice that the data is organized into columns. The different columns illustrate the repetitions that were referred to earlier. Each of the columns corresponds to one  $x, y$  pair, and the variation in height of the data points in these columns is determined by the controllable temperatures. Since only one other PM was involved,  $R_z$ , this repetition did not cause a problem.

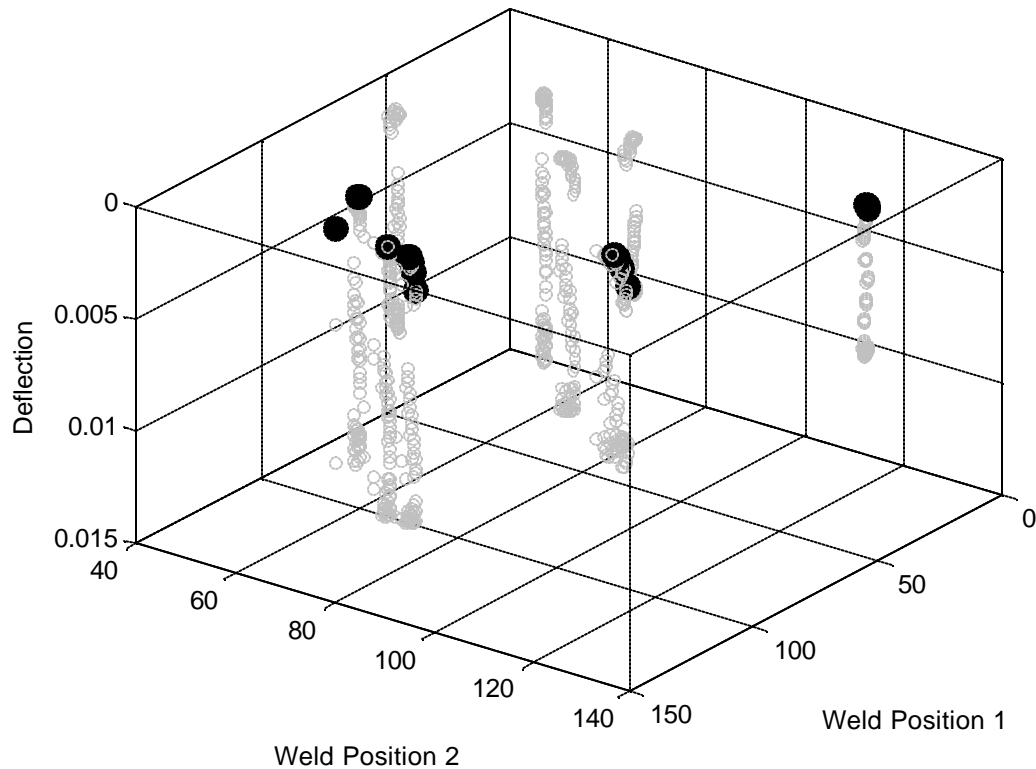


**Figure 4.10:** Visualization of the efficient frontier for the part quality application

**Figure 4.11** shows the efficient solutions with respect to the values of the PMs in increasing order of  $d_1$ . Notice that the compromise between  $d_1$  and  $d_2$  is again evident.

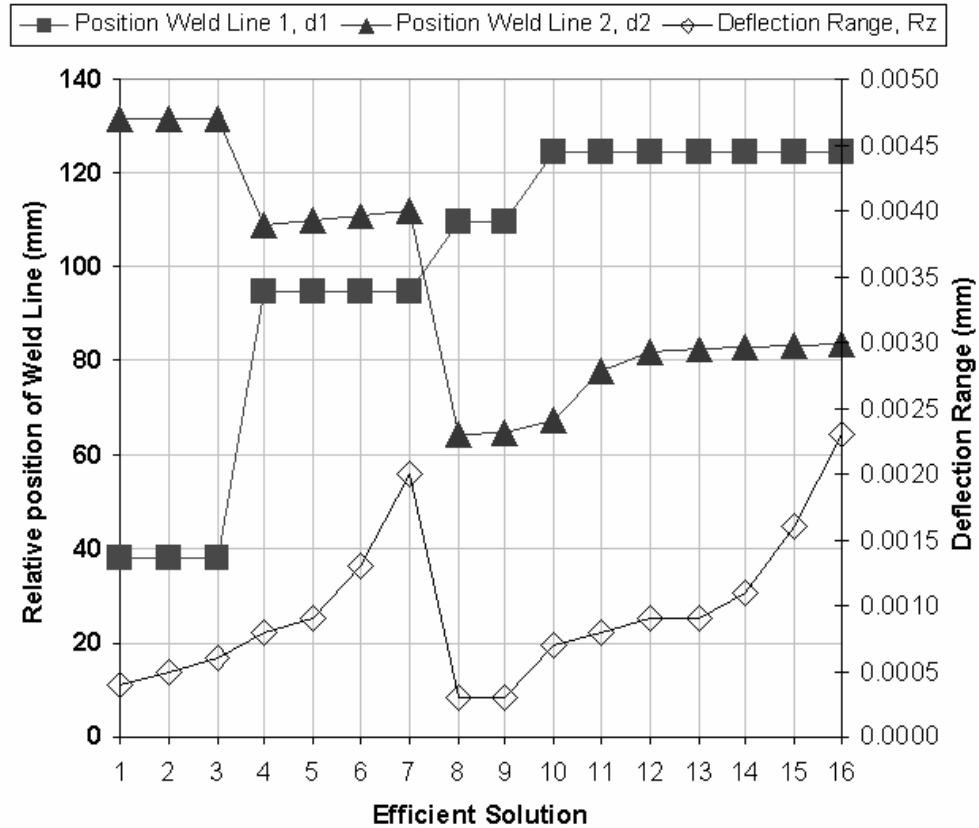


**Figure 4.11:** Efficient solutions for the part quality application in terms of the position of the weld lines and deflection range.

**Figure 4.12** analyzes the clusters of the design variables  $x$  and  $y$ . Again, the entire space shown is the feasible area for the injection gate. This case did not use the same fine grid for the injection location that was used in the structural application, so the ‘attractive’ clusters are not as well defined. However, it is evident that the right and bottom edges would be the best areas to locate the injection gate. This case agrees with the previous cases of the large machine capacity, and the structural application.

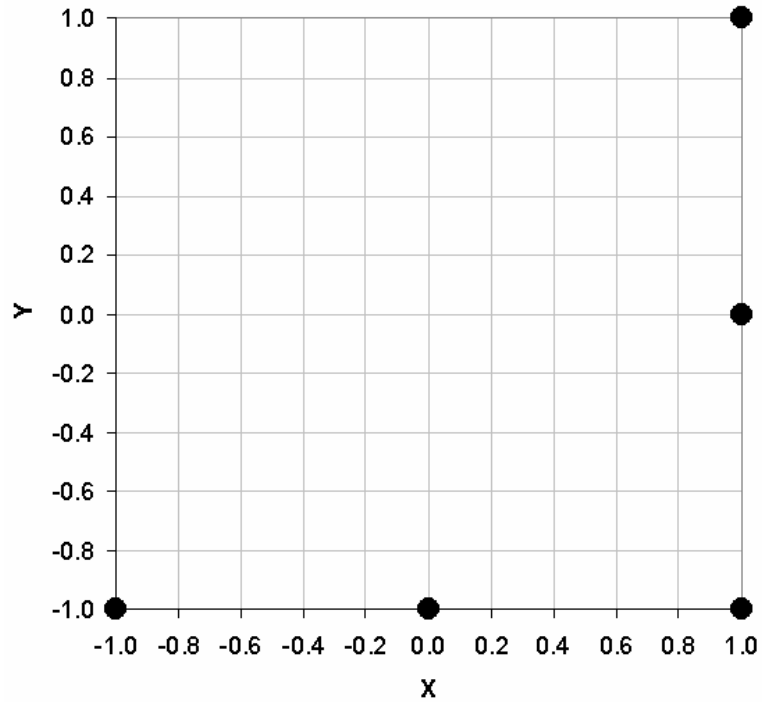


**Figure 4.12:** Injection Locations of the seven efficient solutions to the part quality application transformed to fall between -1 and 1.

**Table 4.7** shows the levels of the controllable variables that correspond to the efficient combinations of PMs. Notice that for all of the efficient solutions, the value of  $T_e$  was 149 degrees C. Allowing the part to cool to a lower ejection temperature favorably affects the part deflection in the z direction. In this case, the time to freeze was not considered. Allowing the part to cool longer did not introduce any negative effects, so the efficient ejection temperature was always at the minimum of the range.

**Table 4.7:** Efficient solutions for the quality critical application

Controllable Variables					Performance Measures		
$X$	$Y$	$T_m$	$T_w$	$T_e$	$R_z$	$d_1$	$d_2$
<i>cm</i>	<i>cm</i>	<i>C</i>	<i>C</i>	<i>C</i>	<i>mm</i>	<i>mm</i>	<i>mm</i>
15	10	130	260	149	0.0003	109.7	64.4
15	10	135	260	149	0.0003	109.7	64.7
20	10	120	260	149	0.0007	124.6	67.4
20	10	130	260	149	0.0008	124.6	77.8
25	10	120	260	149	0.0009	124.7	82.1
25	10	125	260	149	0.0009	124.7	82.5
25	17.5	125	260	149	0.0008	94.9	108.9
25	25	125	260	149	0.0004	37.9	131.4
25	10	130	260	149	0.0011	124.7	82.9
25	17.5	130	260	149	0.0009	94.9	110.0
25	25	130	267.5	149	0.0005	37.9	131.6
25	25	130	275	149	0.0006	37.9	131.6
25	10	135	260	149	0.0016	124.7	83.3
25	17.5	135	260	149	0.0013	94.9	110.9
25	10	140	260	149	0.0023	124.7	83.6
25	17.5	140	260	149	0.0020	94.9	111.8

*Injection Location Dependent Performance Measures:*

From the results of the analysis of variance we can see that there are some PMs that are dependent only on the location of the injection gate. These PMs,  $t_A$ ,  $t_B$ ,  $t_{oe}$ ,  $d_1$ , and  $d_2$ , were considered in a separate case that is only concerned with determining the location of the injection gate. For this case the factorial enumeration of the levels of the controllable variables shown in **Table 4.6** was used. Again because of the high dimensionality of this case, a simplified DEA model (setting the constant  $m_0$  equal to zero) was used. The resulting fourteen efficient solutions are shown in **Figure 4.13**.

Notice the compromises between the time to touch hole A and the time to touch the outer edge. The peaks of these two PMs always contrast each other. On the other hand, the trend of the time to touch hole B follows a similar path as the time to touch hole A. As observed before the compromise between the weld line positions is evident.

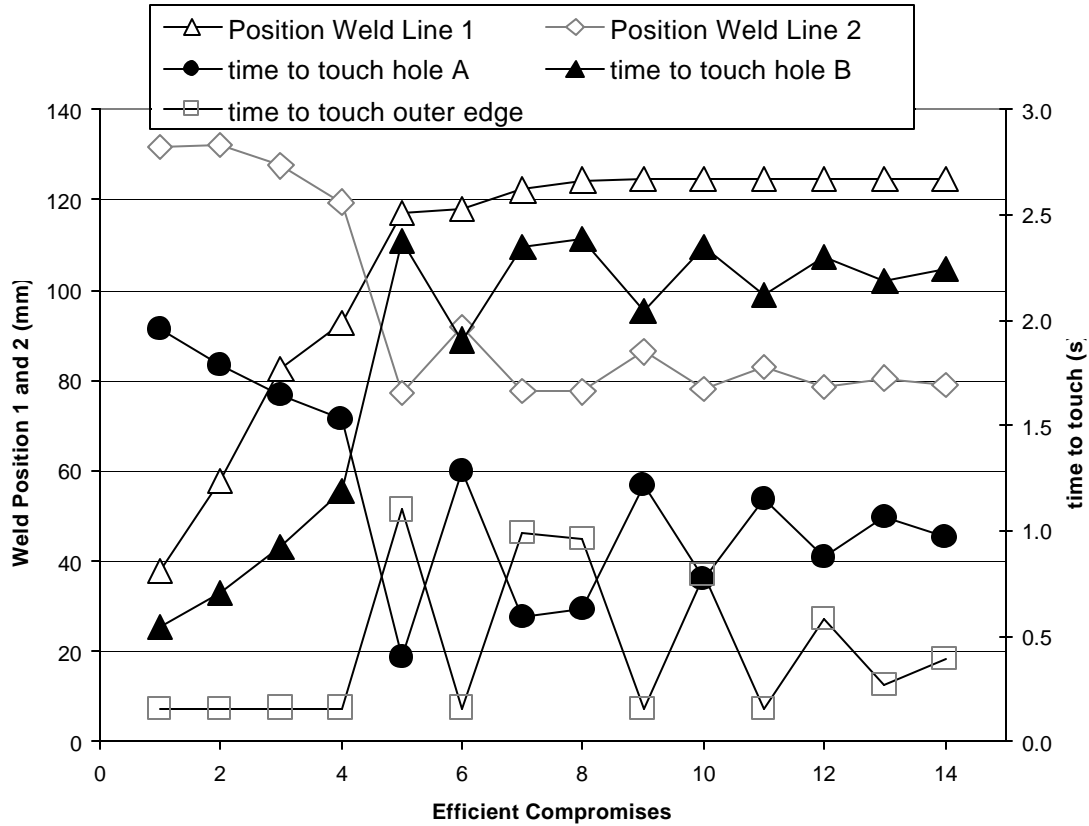


**Figure 4.13:** Efficient solutions for the case of determining the injection location in terms of the levels of the PMs considered.

The efficient gate locations for this case are shown in **Figure 4.14**. This case agreed with some of the earlier cases. The ‘attractive’ clusters for the injection gate occurred along the bottom and right edges. Only a few new injection locations resulted

from introducing the flow times into this case on top of the weld line locations, which were previously considered by themselves in the structural applications. Additionally, these new injection locations are still in the same general area. This implies that generally, the flow times as a group do not introduce definite compromises with respect to the location of the injection gate with the locations of the weld lines. Here the efficient solutions are only dependent on  $x$  and  $y$ , so the levels of the temperatures are not shown.

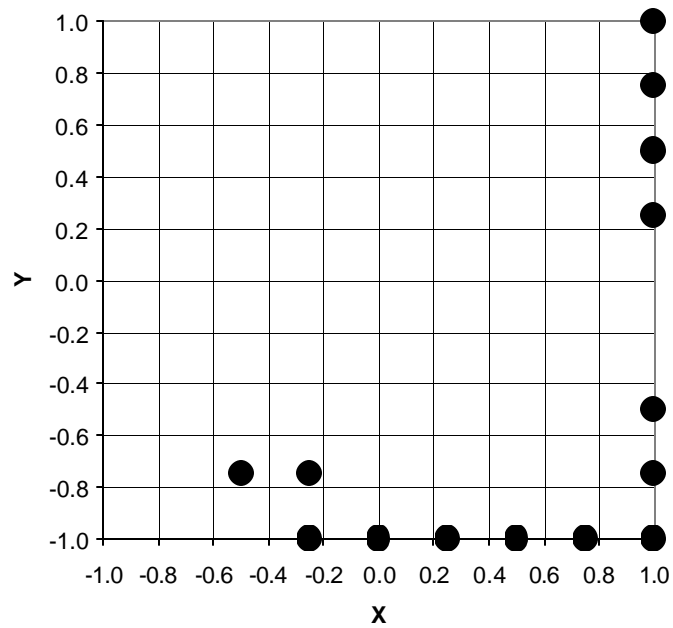


**Figure 4.14:** Injection Locations of the efficient solutions for the application considering only  $x,y$  dependent PMs

### 4.3 Analysis of Robust Solutions:

The discussion of the different cases in the previous section leads to an additional analysis: finding robust efficient solutions. Robust solutions can be found within the individual cases, and some of those were discussed previously. As it can be inferred, a robust efficient solution is a combination of controllable variable settings that remains

efficient when analyzing different subsets of performance measures. It is also beneficial to determine which solutions were robust on a large scale, that is which combinations of process variables were deemed efficient in several subsets of optimization. Indeed for this case it was possible to identify that the combination of  $(x, y, T_m, T_w, T_e) = (20 \text{ cm}, 10 \text{ cm}, 120 \text{ }^\circ\text{C}, 260 \text{ }^\circ\text{C}, 149 \text{ }^\circ\text{C})$  is a robust efficient solution.

Most times determining a suitable location for the injection gate is the most crucial decision. The temperatures at which the process is run can be adjusted easily. On the otherhand, there is only one chance to decide where the injection gate will be located. Selecting the proper location from the start can save a lot of time and money. In this study, it was identified that the injection gate location at the top right corner of the feasible injection area ( $x=20 \text{ cm}, y=25 \text{ cm}$ ) is a robust solution. This injection location was found in efficient solutions for all but one of the subsets, and it was very close to the ‘attractive’ area in the subset in which it did not appear.

This analysis might help to establish a ‘common ground’ among multiple decision makers, to then move to the kind of compromises that can be taken when presented with the rest of the efficient solutions [11].

## Chapter 5

### CONCLUSIONS AND FUTURE WORK

#### 5.1 Conclusions:

Finding the settings of process and design variables in Injection Molding has been an active area of research. In this work, we demonstrated the coordinated use of CAE, statistics, neural networks, and data envelopment analysis has been demonstrated to find these settings in a multiple objective optimization context. A case study was presented to apply the optimization strategy, and additional sub cases were defined to further the details of practical applications in the industry.

The analyses presented in this situation are geared towards making informed decisions on the compromises of several performance measures. It is our premise that characterizing the efficient solutions is an important way to realize the potential of an IM operation [11].

#### 5.2 Future Work:

The future work of this project will involve analyzing the effects of variability on the efficient solutions. In experimental work, there is indefinitely a degree of uncertainty that applies to the input variables. For example, the temperature of the mold might be set at 120 degrees C, but for a particular application, the real value might be the nominal value plus or minus five degrees. This variance could add new compromises and change the shape of the efficient frontier. This will initially be done by introducing artificial variance using the metamodels obtained for the PMs, and using DEA to determine any

changes in the efficient solutions. The goal will be to determine the benefits of the degree at which one is able to control the process.

The next step would be to follow a similar process using experimental data from a real mold. New PMs will be used for the new experimental case. The physical system of interest will be an ASTM standard mold shown in Figure 5.1. One of the PMs to be subject of the variance study is part weight.

## References

- [1] Osswald, T., Sheng, L., Gramann, P.J., *Injection Molding Handbook*. Munich. Hanser (2002)
- [2] Cabrera-Rios, M., Zuyev, K., Chen, X., Castro, J.M., and Straus, E.J. *Polymer Composites*, 23:5 (2002)
- [3] Cabrera-Rios, M., Mount-Campbell, C.A., and Castro J. M. *Journal of Polymer Engineering*, 22:5 (2002)
- [4] Malloy, Robert. *Plastic Part Design for Injection Molding*. Cincinnati: Hanser Gardner, (1994)
- [5] Cabrera Rios, Mauricio. "Multiple Criteria Optimization Studies in Reactive In-Mold Coating." Ph.D. thesis, The Ohio State University, OH, 2002
- [6] Seber, G.A.F., *Linear Regressions Analysis*. New York. John Wiley & Sons (1977)
- [7] Fausset, L., *Fundamentals of Neural Networks: Architectures, Algorithms, and Applications*. Upper Saddle River. Prentice Hall (1994)
- [8] Castro, C.E., Cabrera-Rios, M., Lilly, B., Castro, J.M., and Mount-Campbell, C.A. *Journal of Integrated Design & Process Science*, 7:1 (2003)
- [9] Castro, C.E., Bhagavatula, N., Cabrera-Rios, M., Lilly, B., and Castro, J.M., *ANTEC Proceedings* (2003)
- [10] Charnes, A., Cooper, W.W., Lewin, A.Y., and Seiford, L.M. Boston, Kluwer Academic Publishers (1993)
- [11] Castro, C.E., Cabrera-Rios, M., Lilly, B., and Castro, J.M., *ANTEC Proceedings* (2004)
- [12] Charnes, A., W.W., and Rhodes, E. (1978). *European Journal*

# Appendix A

## Initial Dataset from Moldflow Simulations

	$x$	$y$	$T_w$	$T_m$	$T_e$	$P_l$	$S_w$	$t_l$	$R_z$	$t_A$	$t_B$	$t_{oe}$
1	-0.87	-0.93	-1.00	-1.00	-1.00	30.37	0.15	20.91	0.0008	0.16	2.35	0.76
2	-0.87	-0.93	-1.00	-1.00	1.00	30.37	0.15	17.16	0.0104	0.16	2.35	0.76
3	-0.87	-0.93	-1.00	0.00	-1.00	24.43	0.13	21.91	0.0008	0.16	2.43	0.76
4	-0.87	-0.93	-1.00	0.00	1.00	24.43	0.13	18.41	0.0112	0.16	2.43	0.76
5	-0.87	-0.93	-1.00	1.00	-1.00	19.78	0.11	22.66	0.0008	0.16	2.43	0.76
6	-0.87	-0.93	-1.00	1.00	1.00	19.78	0.11	19.16	0.0119	0.16	2.43	0.76
7	-0.87	-0.93	0.00	-1.00	-1.00	29.11	0.15	25.41	0.0009	0.16	2.43	0.76
8	-0.87	-0.93	0.00	-1.00	1.00	29.11	0.15	19.91	0.0111	0.16	2.43	0.76
9	-0.87	-0.93	0.00	0.00	-1.00	23.45	0.12	26.66	0.0008	0.16	2.43	0.76
10	-0.87	-0.93	0.00	0.00	1.00	23.45	0.12	21.16	0.0125	0.16	2.43	0.76
11	-0.87	-0.93	0.00	1.00	-1.00	19.07	0.11	27.41	0.0010	0.16	2.43	0.76
12	-0.87	-0.93	0.00	1.00	1.00	19.07	0.11	21.91	0.0127	0.16	2.43	0.76
13	-0.87	-0.93	1.00	-1.00	-1.00	27.83	0.14	35.66	0.0020	0.16	2.43	0.76
14	-0.87	-0.93	1.00	-1.00	1.00	27.83	0.14	24.41	0.0115	0.16	2.43	0.76
15	-0.87	-0.93	1.00	0.00	-1.00	22.43	0.12	36.66	0.0019	0.16	2.42	0.76
16	-0.87	-0.93	1.00	0.00	1.00	22.43	0.12	25.66	0.0122	0.16	2.42	0.76
17	-0.87	-0.93	1.00	1.00	-1.00	18.34	0.10	37.91	0.0026	0.16	2.42	0.76
18	-0.87	-0.93	1.00	1.00	1.00	18.34	0.10	26.66	0.0125	0.16	2.42	0.76
19	-1.00	-0.08	-1.00	-1.00	-1.00	27.56	0.15	20.91	0.0007	0.20	2.02	1.26
20	-1.00	-0.08	-1.00	-1.00	1.00	27.56	0.15	17.41	0.0087	0.20	2.02	1.26
21	-1.00	-0.08	-1.00	0.00	-1.00	22.05	0.13	21.91	0.0009	0.20	2.02	1.26
22	-1.00	-0.08	-1.00	0.00	1.00	22.05	0.13	18.41	0.0120	0.20	2.02	1.26
23	-1.00	-0.08	-1.00	1.00	-1.00	17.70	0.11	22.66	0.0008	0.20	2.02	1.27
24	-1.00	-0.08	-1.00	1.00	1.00	17.70	0.11	19.16	0.0133	0.20	2.02	1.27
25	-1.00	-0.08	0.00	-1.00	-1.00	26.37	0.15	25.41	0.0007	0.20	2.03	1.27
26	-1.00	-0.08	0.00	-1.00	1.00	26.37	0.15	19.91	0.0100	0.20	2.03	1.27
27	-1.00	-0.08	0.00	0.00	-1.00	21.08	0.13	26.66	0.0007	0.20	1.95	1.26
28	-1.00	-0.08	0.00	0.00	1.00	21.08	0.13	20.91	0.0106	0.20	1.95	1.26
29	-1.00	-0.08	0.00	1.00	-1.00	16.98	0.11	27.41	0.0008	0.19	2.02	1.26
30	-1.00	-0.08	0.00	1.00	1.00	16.98	0.11	21.91	0.0146	0.19	2.02	1.26
31	-1.00	-0.08	1.00	-1.00	-1.00	25.23	0.15	35.66	0.0014	0.20	2.02	1.26
32	-1.00	-0.08	1.00	-1.00	1.00	25.23	0.15	24.41	0.0105	0.20	2.02	1.26
33	-1.00	-0.08	1.00	0.00	-1.00	20.20	0.13	36.91	0.0008	0.20	2.02	1.26
34	-1.00	-0.08	1.00	0.00	1.00	20.20	0.13	25.66	0.0143	0.20	2.02	1.26
35	-1.00	-0.08	1.00	1.00	-1.00	16.41	0.11	37.91	0.0022	0.19	2.02	1.26
36	-1.00	-0.08	1.00	1.00	1.00	16.41	0.11	26.66	0.0154	0.19	2.02	1.26
37	-0.81	0.93	-1.00	-1.00	-1.00	19.63	0.14	20.91	0.0006	1.06	0.68	0.38
38	-0.81	0.93	-1.00	-1.00	1.00	19.63	0.14	17.16	0.0098	1.06	0.68	0.38
39	-0.81	0.93	-1.00	0.00	-1.00	15.45	0.11	21.91	0.0006	1.05	0.67	0.38
40	-0.81	0.93	-1.00	0.00	1.00	15.45	0.11	18.16	0.0098	1.05	0.67	0.38
41	-0.81	0.93	-1.00	1.00	-1.00	12.20	0.09	22.66	0.0006	1.05	0.67	0.38
42	-0.81	0.93	-1.00	1.00	1.00	12.20	0.09	19.16	0.0096	1.05	0.67	0.38
43	-0.81	0.93	0.00	-1.00	-1.00	18.87	0.14	25.41	0.0007	1.05	0.68	0.38
44	-0.81	0.93	0.00	-1.00	1.00	18.87	0.14	19.91	0.0099	1.05	0.68	0.38
45	-0.81	0.93	0.00	0.00	-1.00	14.73	0.11	26.41	0.0008	1.05	0.67	0.38
46	-0.81	0.93	0.00	0.00	1.00	14.73	0.11	20.91	0.0097	1.05	0.67	0.38
47	-0.81	0.93	0.00	1.00	-1.00	11.67	0.09	27.41	0.0008	1.05	0.67	0.38
48	-0.81	0.93	0.00	1.00	1.00	11.67	0.09	21.91	0.0095	1.05	0.67	0.38
49	-0.81	0.93	1.00	-1.00	-1.00	17.91	0.14	35.66	0.0020	1.05	0.68	0.38
50	-0.81	0.93	1.00	-1.00	1.00	17.91	0.14	24.41	0.0097	1.05	0.68	0.38
51	-0.81	0.93	1.00	0.00	-1.00	13.99	0.11	36.66	0.0019	1.05	0.67	0.38
52	-0.81	0.93	1.00	0.00	1.00	13.99	0.11	25.66	0.0095	1.05	0.67	0.38
53	-0.81	0.93	1.00	1.00	-1.00	11.18	0.09	37.91	0.0020	1.05	0.67	0.38
54	-0.81	0.93	1.00	1.00	1.00	11.18	0.09	26.66	0.0094	1.05	0.67	0.38

**Table A.1:** Initial dataset used to fit metamodells obtained from Moldflow simulations

Continued

Appendix 1 Continued

55	0.21	-1.00	-1.00	-1.00	-1.00	30.72	0.16	20.91	0.0007	0.86	2.31	0.61
56	0.21	-1.00	-1.00	-1.00	1.00	30.72	0.16	17.41	0.0100	0.86	2.31	0.61
57	0.21	-1.00	-1.00	0.00	-1.00	24.68	0.14	21.91	0.0007	0.85	2.30	0.61
58	0.21	-1.00	-1.00	0.00	1.00	24.68	0.14	18.41	0.0114	0.85	2.30	0.61
59	0.21	-1.00	-1.00	1.00	-1.00	19.97	0.12	22.91	0.0007	0.86	2.30	0.61
60	0.21	-1.00	-1.00	1.00	1.00	19.97	0.12	19.16	0.0118	0.86	2.30	0.61
61	0.21	-1.00	0.00	-1.00	-1.00	29.44	0.15	25.66	0.0009	0.86	2.32	0.62
62	0.21	-1.00	0.00	-1.00	1.00	29.44	0.15	19.91	0.0111	0.86	2.32	0.62
63	0.21	-1.00	0.00	0.00	-1.00	23.67	0.13	26.66	0.0008	0.87	2.30	0.61
64	0.21	-1.00	0.00	0.00	1.00	23.67	0.13	20.91	0.0117	0.87	2.30	0.61
65	0.21	-1.00	0.00	1.00	-1.00	19.30	0.11	27.41	0.0008	0.87	2.30	0.61
66	0.21	-1.00	0.00	1.00	1.00	19.30	0.11	21.91	0.0121	0.87	2.30	0.61
67	0.21	-1.00	1.00	-1.00	-1.00	27.98	0.15	35.66	0.0021	0.87	2.30	0.61
68	0.21	-1.00	1.00	-1.00	1.00	27.98	0.15	24.66	0.0117	0.87	2.30	0.61
69	0.21	-1.00	1.00	0.00	-1.00	22.66	0.13	36.66	0.0022	0.87	2.30	0.61
70	0.21	-1.00	1.00	0.00	1.00	22.66	0.13	25.66	0.0119	0.87	2.30	0.61
71	0.21	-1.00	1.00	1.00	-1.00	18.45	0.11	37.91	0.0027	0.85	2.30	0.61
72	0.21	-1.00	1.00	1.00	1.00	18.45	0.11	26.66	0.0122	0.85	2.30	0.61
73	0.12	0.00	-1.00	-1.00	-1.00	27.22	0.17	20.91	0.0012	0.94	1.82	0.70
74	0.12	0.00	-1.00	-1.00	1.00	27.22	0.17	17.16	0.0105	0.94	1.82	0.70
75	0.12	0.00	-1.00	0.00	-1.00	21.58	0.14	21.91	0.0010	0.94	1.82	0.70
76	0.12	0.00	-1.00	0.00	1.00	21.58	0.14	18.41	0.0119	0.94	1.82	0.70
77	0.12	0.00	-1.00	1.00	-1.00	17.32	0.12	22.66	0.0012	0.94	1.81	0.70
78	0.12	0.00	-1.00	1.00	1.00	17.32	0.12	19.16	0.0118	0.94	1.81	0.70
79	0.12	0.00	0.00	-1.00	-1.00	26.00	0.17	25.41	0.0010	0.94	1.81	0.70
80	0.12	0.00	0.00	-1.00	1.00	26.00	0.17	19.91	0.0118	0.94	1.81	0.70
81	0.12	0.00	0.00	0.00	-1.00	20.48	0.14	26.66	0.0011	0.94	1.81	0.70
82	0.12	0.00	0.00	0.00	1.00	20.48	0.14	20.91	0.0123	0.94	1.81	0.70
83	0.12	0.00	0.00	1.00	-1.00	16.51	0.12	27.41	0.0009	0.93	1.82	0.70
84	0.12	0.00	0.00	1.00	1.00	16.51	0.12	21.91	0.0124	0.93	1.82	0.70
85	0.12	0.00	1.00	-1.00	-1.00	24.68	0.16	35.66	0.0018	0.93	1.82	0.70
86	0.12	0.00	1.00	-1.00	1.00	24.68	0.16	24.41	0.0125	0.93	1.82	0.70
87	0.12	0.00	1.00	0.00	-1.00	19.54	0.14	36.66	0.0017	0.93	1.82	0.70
88	0.12	0.00	1.00	0.00	1.00	19.54	0.14	25.66	0.0124	0.93	1.82	0.70
89	0.12	0.00	1.00	1.00	-1.00	15.84	0.12	37.91	0.0023	0.93	1.82	0.70
90	0.12	0.00	1.00	1.00	1.00	15.84	0.12	26.66	0.0129	0.93	1.82	0.70
91	0.15	0.85	-1.00	-1.00	-1.00	25.74	0.14	20.91	0.0008	1.52	0.80	0.69
92	0.15	0.85	-1.00	-1.00	1.00	25.74	0.14	17.41	0.0074	1.52	0.80	0.69
93	0.15	0.85	-1.00	0.00	-1.00	20.57	0.12	21.91	0.0010	1.52	0.79	0.68
94	0.15	0.85	-1.00	0.00	1.00	20.57	0.12	18.41	0.0073	1.52	0.79	0.68
95	0.15	0.85	-1.00	1.00	-1.00	16.50	0.10	22.66	0.0008	1.52	0.79	0.68
96	0.15	0.85	-1.00	1.00	1.00	16.50	0.10	19.16	0.0072	1.52	0.79	0.68
97	0.15	0.85	0.00	-1.00	-1.00	24.91	0.15	25.41	0.0009	1.51	0.78	0.68
98	0.15	0.85	0.00	-1.00	1.00	24.91	0.15	19.91	0.0074	1.51	0.78	0.68
99	0.15	0.85	0.00	0.00	-1.00	19.87	0.12	26.66	0.0010	1.50	0.78	0.67
100	0.15	0.85	0.00	0.00	1.00	19.87	0.12	20.91	0.0073	1.50	0.78	0.67
101	0.15	0.85	0.00	1.00	-1.00	15.96	0.10	27.41	0.0009	1.50	0.78	0.67
102	0.15	0.85	0.00	1.00	1.00	15.96	0.10	21.91	0.0073	1.50	0.78	0.67
103	0.15	0.85	1.00	-1.00	-1.00	23.76	0.14	35.66	0.0018	1.50	0.78	0.68
104	0.15	0.85	1.00	-1.00	1.00	23.76	0.14	24.41	0.0074	1.50	0.78	0.68
105	0.15	0.85	1.00	0.00	-1.00	18.59	0.12	36.91	0.0020	1.50	0.78	0.68
106	0.15	0.85	1.00	0.00	1.00	18.59	0.12	25.66	0.0074	1.50	0.78	0.68
107	0.15	0.85	1.00	1.00	-1.00	15.47	0.10	37.91	0.0023	1.50	0.78	0.67
108	0.15	0.85	1.00	1.00	1.00	15.47	0.10	26.66	0.0074	1.50	0.78	0.67

Continued

Appendix 1 Continued

109	1.00	-0.98	-1.00	-1.00	-1.00	30.99	0.16	20.91	0.0006	1.16	2.13	0.16
110	1.00	-0.98	-1.00	-1.00	1.00	30.99	0.16	17.16	0.0127	1.16	2.13	0.16
111	1.00	-0.98	-1.00	0.00	-1.00	24.98	0.14	21.91	0.0009	1.16	2.12	0.16
112	1.00	-0.98	-1.00	0.00	1.00	24.98	0.14	18.41	0.0138	1.16	2.12	0.16
113	1.00	-0.98	-1.00	1.00	-1.00	20.16	0.12	22.66	0.0009	1.15	2.12	0.16
114	1.00	-0.98	-1.00	1.00	1.00	20.16	0.12	19.16	0.0139	1.15	2.12	0.16
115	1.00	-0.98	0.00	-1.00	-1.00	29.64	0.16	25.41	0.0008	1.15	2.12	0.16
116	1.00	-0.98	0.00	-1.00	1.00	29.64	0.16	19.91	0.0129	1.15	2.12	0.16
117	1.00	-0.98	0.00	0.00	-1.00	23.83	0.13	26.66	0.0010	1.16	2.12	0.16
118	1.00	-0.98	0.00	0.00	1.00	23.83	0.13	20.91	0.0134	1.16	2.12	0.16
119	1.00	-0.98	0.00	1.00	-1.00	19.39	0.11	27.41	0.0015	1.15	2.11	0.15
120	1.00	-0.98	0.00	1.00	1.00	19.39	0.11	21.91	0.0138	1.15	2.11	0.15
121	1.00	-0.98	1.00	-1.00	-1.00	28.09	0.15	35.66	0.0023	1.15	2.11	0.16
122	1.00	-0.98	1.00	-1.00	1.00	28.09	0.15	24.41	0.0126	1.15	2.11	0.16
123	1.00	-0.98	1.00	0.00	-1.00	22.87	0.13	36.66	0.0026	1.15	2.11	0.16
124	1.00	-0.98	1.00	0.00	1.00	22.87	0.13	25.66	0.0130	1.15	2.11	0.16
125	1.00	-0.98	1.00	1.00	-1.00	18.50	0.11	37.91	0.0032	1.15	2.11	0.15
126	1.00	-0.98	1.00	1.00	1.00	18.50	0.11	26.66	0.0141	1.15	2.11	0.15
127	0.85	-0.18	-1.00	-1.00	-1.00	27.45	0.17	20.91	0.0009	1.32	1.72	0.24
128	0.85	-0.18	-1.00	-1.00	1.00	27.45	0.17	17.16	0.0106	1.32	1.72	0.24
129	0.85	-0.18	-1.00	0.00	-1.00	21.86	0.14	21.91	0.0010	1.31	1.72	0.23
130	0.85	-0.18	-1.00	0.00	1.00	21.86	0.14	18.41	0.0108	1.31	1.72	0.23
131	0.85	-0.18	-1.00	1.00	-1.00	17.50	0.12	22.66	0.0011	1.31	1.71	0.23
132	0.85	-0.18	-1.00	1.00	1.00	17.50	0.12	19.16	0.0105	1.31	1.71	0.23
133	0.85	-0.18	0.00	-1.00	-1.00	26.28	0.17	25.41	0.0010	1.31	1.72	0.23
134	0.85	-0.18	0.00	-1.00	1.00	26.28	0.17	19.91	0.0106	1.31	1.72	0.23
135	0.85	-0.18	0.00	0.00	-1.00	20.85	0.14	26.66	0.0010	1.31	1.71	0.23
136	0.85	-0.18	0.00	0.00	1.00	20.85	0.14	20.91	0.0106	1.31	1.71	0.23
137	0.85	-0.18	0.00	1.00	-1.00	16.74	0.12	27.41	0.0009	1.32	1.71	0.23
138	0.85	-0.18	0.00	1.00	1.00	16.74	0.12	21.91	0.0106	1.32	1.71	0.23
139	0.85	-0.18	1.00	-1.00	-1.00	24.96	0.16	35.66	0.0018	1.32	1.71	0.23
140	0.85	-0.18	1.00	-1.00	1.00	24.96	0.16	24.41	0.0107	1.32	1.71	0.23
141	0.85	-0.18	1.00	0.00	-1.00	19.83	0.13	36.91	0.0021	1.31	1.71	0.23
142	0.85	-0.18	1.00	0.00	1.00	19.83	0.13	25.66	0.0106	1.31	1.71	0.23
143	0.85	-0.18	1.00	1.00	-1.00	16.10	0.11	37.91	0.0029	1.31	1.71	0.23
144	0.85	-0.18	1.00	1.00	1.00	16.10	0.11	26.66	0.0105	1.31	1.71	0.23
145	0.97	1.00	-1.00	-1.00	-1.00	27.15	0.14	20.91	0.0009	1.95	0.56	0.18
146	0.97	1.00	-1.00	-1.00	1.00	27.15	0.14	17.41	0.0070	1.95	0.56	0.18
147	0.97	1.00	-1.00	0.00	-1.00	21.84	0.11	21.91	0.0009	1.95	0.55	0.17
148	0.97	1.00	-1.00	0.00	1.00	21.84	0.11	18.41	0.0070	1.95	0.55	0.17
149	0.97	1.00	-1.00	1.00	-1.00	17.55	0.09	22.66	0.0008	1.95	0.55	0.17
150	0.97	1.00	-1.00	1.00	1.00	17.55	0.09	19.16	0.0071	1.95	0.55	0.17
151	0.97	1.00	0.00	-1.00	-1.00	26.44	0.13	25.41	0.0011	1.95	0.55	0.18
152	0.97	1.00	0.00	-1.00	1.00	26.44	0.13	19.91	0.0069	1.95	0.55	0.18
153	0.97	1.00	0.00	0.00	-1.00	20.96	0.11	26.66	0.0010	1.95	0.55	0.17
154	0.97	1.00	0.00	0.00	1.00	20.96	0.11	20.91	0.0070	1.95	0.55	0.17
155	0.97	1.00	0.00	1.00	-1.00	16.79	0.09	27.41	0.0012	1.95	0.55	0.17
156	0.97	1.00	0.00	1.00	1.00	16.79	0.09	21.91	0.0071	1.95	0.55	0.17
157	0.97	1.00	1.00	-1.00	-1.00	25.40	0.14	35.66	0.0025	1.95	0.55	0.17
158	0.97	1.00	1.00	-1.00	1.00	25.40	0.14	24.41	0.0070	1.95	0.55	0.17
159	0.97	1.00	1.00	0.00	-1.00	20.19	0.11	36.91	0.0022	1.95	0.55	0.17
160	0.97	1.00	1.00	0.00	1.00	20.19	0.11	25.66	0.0071	1.95	0.55	0.17
161	0.97	1.00	1.00	1.00	-1.00	16.44	0.09	37.91	0.0026	1.95	0.55	0.17
162	0.97	1.00	1.00	1.00	1.00	16.44	0.09	26.66	0.0072	1.95	0.55	0.17